ORIGINAL ARTICLE

Simulation of the effect of salinity-clay variation on the electrical potential of the quaternary aquifer using multiphysics modeling

A. I. Ammar[1,2] · A. S. A. Abu El-Ata[3] · A. A. Mustafa[1] · K. A. Kamal[1] · Amir M. S. Lala[3]

Abstract

Salinity and clay content are effective factors in influencing the hydro-geoelectric properties of porous rocks, such as electrical conductivity. The COMSOL Multiphysics model was used in this study to simulate this parameter, to realize the effect of the variation of salinity and clay on the electrical potential of the Quaternary aquifer in the fresh groundwater zone, brackish groundwater zone and saline groundwater zone across the middle Nile Delta of Egypt, by applying the Direct Current resistivity method. The electrical model included four different geological layers in lithology and resistivities. Nine VESes were performed to calculate the electrical potential and the apparent resistivity of these layers, focusing on the Quaternary aquifer. The coefficient of decreasing and rate of decreasing in the electrical potential were calculated and it was found that it reflects a weak, medium, and high to very high significant effect of salinity and clay content in the fresh groundwater zone, brackish groundwater zone and saline groundwater zone, respectively. The results indicated the expected errors in resistivity measurements, estimation of hydro-geoelectric parameters and sediments description in the three water zones and the accuracy of their separation. This simulation helped to understanding the effect of salinity-clay variation on the electrical potential of porous sediments. It can, therefore, be considered as an essential step to solve the hydro-geoelectric and environmental problems of aquifers affected by this variation, focusing on clarifying how this variation has reduced the accuracy of the hydro-geoelectric parameters and lithologic description.

Keywords Quaternary aquifer · Salinity-clay variation · Three water zones · Multiphysics modeling · Resistivity simulation · Electrical potential

Introduction

In general, the phenomenon of seawater intrusion is one of many complex hydrogeological problems, due to the salinity change in the chemical and physical properties of porous geological layers, such as aquifers. After 1984, along the Nile delta in Egypt, groundwater salinity began to increase, due to higher withdrawals and reduced Nile flow (Saqr et al. 2004). Several authors have studied this problem and demonstrated that groundwater salinization has an effect on the

Quaternary aquifer through the intrusion of seawater into the groundwater, where the problem persists. Since this phenomenon is a serious problem, it is important to know how salt water, due to seawater intrusion, can affect the different physical properties of these layers, such as the resistivity of layers with different salinities [low (fresh), medium (brackish or slightly saline) and high (salty)] by calculating their electrical potential while passing electric current through them. Also, there are many subsurface geophysical and hydrogeological parameters that cannot be understood using surface geophysical methods. Therefore, the development of Multiphysics models has helped to solve many complex subsurface parameters, whether hydrogeological or geophysical, as these models are becoming more and more applicable in various disciplines of Earth sciences. Therefore, the effect of salinity variation and clay-rich sediments on the electrical potential of the geological layers, during the flow of electric current through them to measure the resistivity of sediments,

✉ A. I. Ammar
Abdallah_ammar@nwrc.gov.eg

1 National Water Research Center, Research Institute for Groundwater, Cairo, Egypt

2 National Water Research Center, Water Resources Research Institute, Cairo, Egypt

3 Geophysics Department, Faculty of Science, Ain-Shams University, Cairo, Egypt

is an important and complex problem in Earth sciences with reference to geophysical problems.

In this study, the COMSOL Multiphysics Numerical Model (CMNM) was used to simulate the mentioned problem, by applying it to the Quaternary Nile Delta (QNDA) aquifer in Egypt, because it has lateral and vertical variation in salinity and sediment contents. The salinity variations have been classified into three regions, the fresh groundwater zone, the brackish (transitional) groundwater zone and the saline groundwater zone. The fresh groundwater zone extends to the south of the middle Nile Delta (MND). The brackish groundwater zone is roughly present across the MND especially in the central part, while the saline to brine groundwater zone, due to the effect of seawater intrusion, is located in the north and increases in salinity in the far north, where the Mediterranean is present. Thus, it is interesting to study and understand the geological and hydrogeological settings of the Nile Delta (ND) in Egypt, focusing on the middle part to accurately determine the parameters of the input model. Figure 1 represents the general map of the area (MND for Egypt).

These days, the Comsol multiphysics model (CMM) has been used in various branches of Earth sciences. Wang et al. (2011) showed an important significance of applying COMSOL Multiphysics in geophysical modeling (DC resistivity method forward modeling). Butler and Sinha (2012) used this model for modeling different geophysical methods and DC resistivity was one such method using an AC/DC module. Electromagnetic methods were carried out by Bulter and Zhang (2016) and Li and Smith (2015) also carried out a radio imaging method using this model. Sanuade et al.

(2021) COMSOL multiphysics can be used to simulate several DC resistivity methods forward modeling problems. Ammar (2021), Comsol version 4.4 (2014) used this model to simulate the resistivity and hydroelectrical characteristics of the fractured rock aquifer, using the 1D Vertical Electrical Sounding (VES) technique and found a reliable solution to the forward modeling resistivity method. Accordingly, this model can be used successfully to study, solve, and understand the hydro-geoelectrical conditions of the different aquifers.

Therefore, in this study, and depending on the expected changes in electrical resistivity or conductivity of saturated subsurface geological sediments, and due to lateral and vertical differences in salinity and clay content from south to north, COMSOL Multiphysics (version 5.4 2018), which uses a finite element approach, will be used to simulate these parameters to understand the effect of salinity and clay content on the electrical potential of the Quaternary Nile Delta aquifer (QNDA). This will be done by calculating the aquifer electrical potential values from S to N across MND in three regions, fresh, brackish and saline, by applying DC resistivity technique. However, these potential values will help in calculating the apparent resistivity values (ρ_a) of the groundwater aquifer and upper sediments. Variation in electrical potential and apparent resistivity values will help in understanding how seawater intrusion affects the chemical properties of sediments, leading to a significant change in their physical properties. This change will be achieved by the electrical potential drop rate and the apparent resistivity. Also, this simulation will be accomplished by plotting electrical potential curves and then apparent resistivity curves
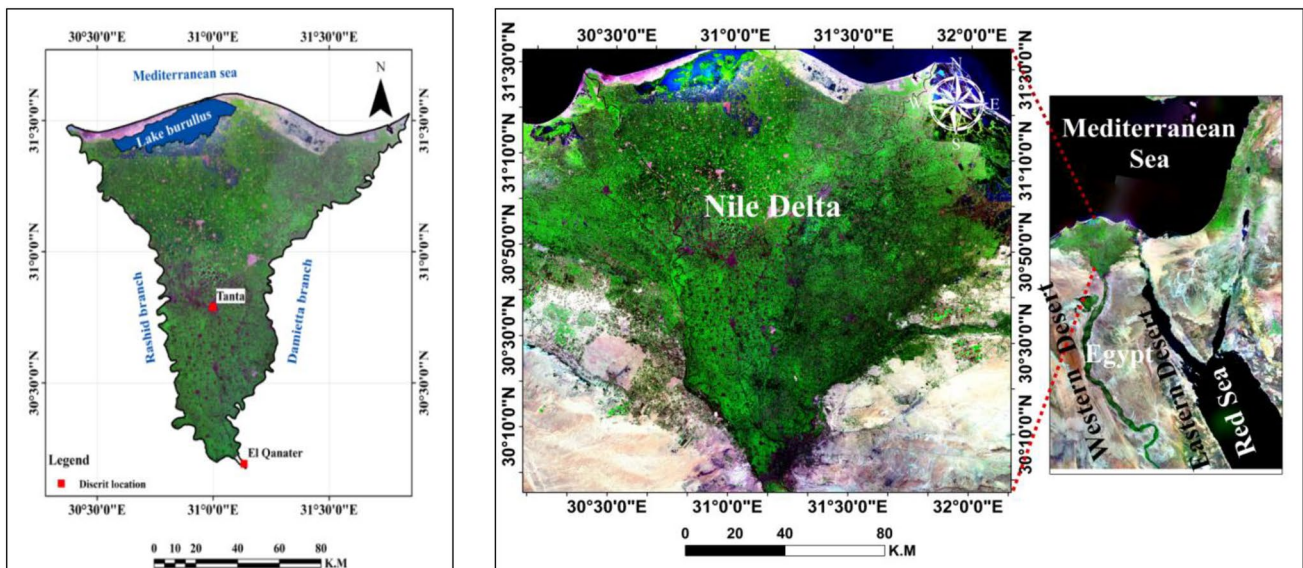
Fig. 1 Satellite images of the location map of the Nile Delta (two panels on the right) and the boundaries of the selected study area in the MND (left panel)

for the Quaternary sediments that include the Quaternary aquifer. Therefore, the comparison of these curves will help in identifying and separating the effects of the three previous salinity zones in the Nile Delta and other related areas. It will also be used in the comparison of measured field curves and expecting the ranges of salinity and clay content.

Description of the selected area

Generally, the selected area, for applying this study, is Nile Delta, Egypt, especially in the MND. The elevation of this part of the ND ranges from zero (at the Mediterranean Sea) up to 32 m (at the civilized land) due to buildings. It ranges between ~ 18 m + msl at El Qanater El Khayreya to the south and ~ 5 m near the city of Tanta with very gently sloping by 1 m/10 km in the northward directions (Shata and El-Fayoumey 1970; Saleh 1980). Geomorphologically, there are three geomorphologic units; *1st unit is the submerged plain of the Mediterranean off-shore* which includes the sites between the coast of Mediterranean and the slope of the outer shelf, at a depth ~ 200 m. *2nd unit is the Mediterranean fore-shore plain* which occupies the coastal lakes. The sabkhas consisting of clays intercalation with sand and silt; the mobile and stable coastal dunes. *3rd unit is the young fluviatile plain*. It is occupying much of the middle part of the ND region and underlain by silt and clay layer. The slope of this plain is very gentle northward by ~ 1 m/10 km.

Geology

In general, the deposits of Quaternary cover the ND region and made up of Nile gravels, sands, clay with sand intercalation, clay and silt. It has a thick sequence of sedimentary layers of Neogene deposits to Quaternary deposits as mentioned by Zaghloul et al. 1977, Said 1981 and Sherif 1999. This sedimentary section overlies the basement complex and attains a thickness of < 3 km. The Quaternary deposits include the deposits of Holocene and Pleistocene age (RIGW 1980). The Tertiary sediments consist of Pliocene, Miocene, Oligocene, Eocene, and Paleocene deposits. The Miocene deposits consist of the formations of Sidi Salim, Qawasim, and Rosetta, its thickness is around 2000 m. The Pliocene–Pleistocene deposits include the formations of Abu Madi, Kafr El Sheikh, El-Wastani, and Mit Ghamr. The Holocene deposits include Bilqas formation. The interesting units, which imply groundwater, are the formations of Mit Ghamr, and El Wastani. (Pleistocene deposits). They considered the Quaternary aquifer and include sand and gravel, where its thickness ranges from 100 to 1000 m at Cairo and at the coast, respectively, along the MND, and decreases to 0 to the west and east of the fringes of ND.

In this study, it will focus on describing the formations of Bilqas, Mit Ghamr, and El-Wastani and Kafr El Sheikh as follow:

- *Bilqas Fm:* It represents the Holocene age, with varying thickness from 25 to 50 m. It is including of sand, with clay or silty clay interbeds (Said 1990; Sherif 1999). It includes clay layer at its base. This layer is considered as the cap layer for the Quaternary aquifer and ranged from 5 m (south) to 74 m (north) in thickness along the MND (Kamal 2000; Sakr 2005) (Fig. 2).
- *Mit Ghamr Fm:* It represents the age of Pleistocene, with varying in thickness, from 463 to 700 m (Schlumberger 1984) and made up of sand and pebble beds, with minor clay (sand and gravel) (Said 1981).
- *El-Wastani Fm:* It is Pleistocene age (from Early to Middle), with thickness of 300 m. It is consisting of sand, with intercalation of clay (Schlumberger 1984; Said 1990). The 3D lithologic model, 3D fence diagram, and 2D cross-section in Fig. 2 show and describe the major Quaternary deposits of the three former formations, with thickness along the MND (from the south to the north).
- *Kafr El Sheikh Fm:* It is Pliocene (from Early to Middle) and made up of clay, with minor sand intercalations and a thickness ranges from 1500 m (Schlumberger 1984) to 1760 m (Said 1981) to 1950 m (Said 1990). This formation is underlying the Quaternary deposits.

Hydrogeology of the quaternary aquifer

Generally, this aquifer occurs in the ND region within a depth range of 50 m from the land surface (Sherif et al. 2012), due to the presence of Holocene deposits. This aquifer is made up of sand and gravel, with varying thickness of lenses of silt and clay (Fig. 2) with high storage capacity and high hydraulic conductivity. Its thickness ranges from 100 to 400 m (south) and an average of 800 m (north) of the ND and in general its thickness ranges from 400 to 1000 m. This aquifer is the considered the main groundwater aquifer in the ND region (Ebraheem et al. 1997). El-Atfy (2007) and MWRI (2013) stated that, its thickness along the MND tract ranges from ˃ 500 m (near Tanta city) and increases to ~ 1000 m to the northward (near the coast). Rizzini et al. (1978), Said (1981), Serag El Din (1989), RIGW (1992), and Dahab (1993) reported that, the thickness of this aquifer ranges from 200 m or 250 m (at the southern parts) to 900 m or 1000 m (at the northern parts).

This aquifer is considered multi-layers' aquifer system, especially in the northern location, that, includes four zones and these zones are separated by three thin clay layers (Hefny 1980; Sallouma 1983; and Serag El Din 1989). These layers have been changed to sand and gravel homogenous facies towards the southern direction (Farid 1980). The
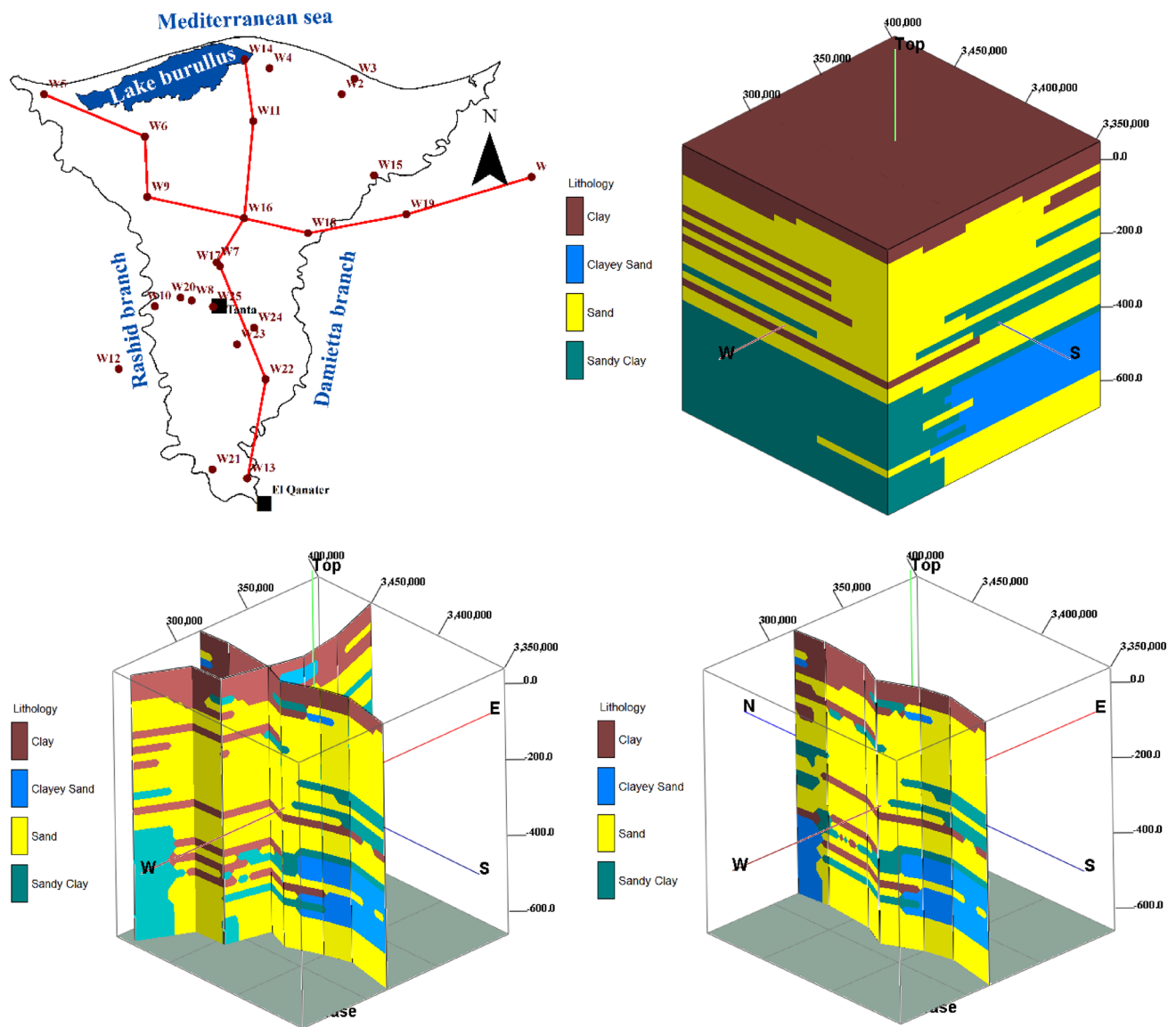
Fig. 2 Shallow wells distribution map of the Quaternary deposits, along the MND, with cross sections (upper left panel), a 3D lithologic model of the Quaternary deposits (upper right panel), a 3D Fence diagram, showing the lithologic description of the Quaternary deposits (lower left panel), and a 2D cross-section, showing the Quaternary deposits from south to north, along the MND (lower right panel) with depth (Z axis) (Rockworks software 15 (Rockware 2011))

average content of clay ranges from 4.5 to 22%, with high intensity of the clay lenses in the northeastern parts (Salem et al. 2008). This aquifer covered by clay cap of the Holocene Bilqas Formation (Fig. 2) (RIGW 1980, 1992; Farid 1980). The groundwater of this layer is in direct contact with the Quaternary aquifer, through upward and downward leakage. It is underlined by impermeable Pliocene shale/clay, with minor sand intercalations of the Kafr El Sheikh Fm (RIGW 1980; Said 1990).

The water level ranges from 6 to 12 m, in the central and southern locations of the ND, from 0 to 5 m in the northern sites. It ranges between 1 and 2 m (north), increases from

3 to 4 m (middle) and reaches 5 m (south) (Schlumberger 1995; CEDARE 2002). In the selected area, saline and brackish water represent ＞ 90% of the groundwater, due to sea water intrusion (Abd-Elhamid et al. 2019). According to kamal (2000), the groundwater depth ranges between 0.1 m (near Lake Burullus) and ~ 7 m (near Tanta city) as shown in Fig. 3, right panel. According to the hydrogeologic map (Fig. 3, left panel), the depth to groundwater table ranged between 1 m (to the south of Lake Burullus, in the northern parts) and 5 m (to the south of Tanta city), (RIGW 1992, 2002; Morsy 2009).
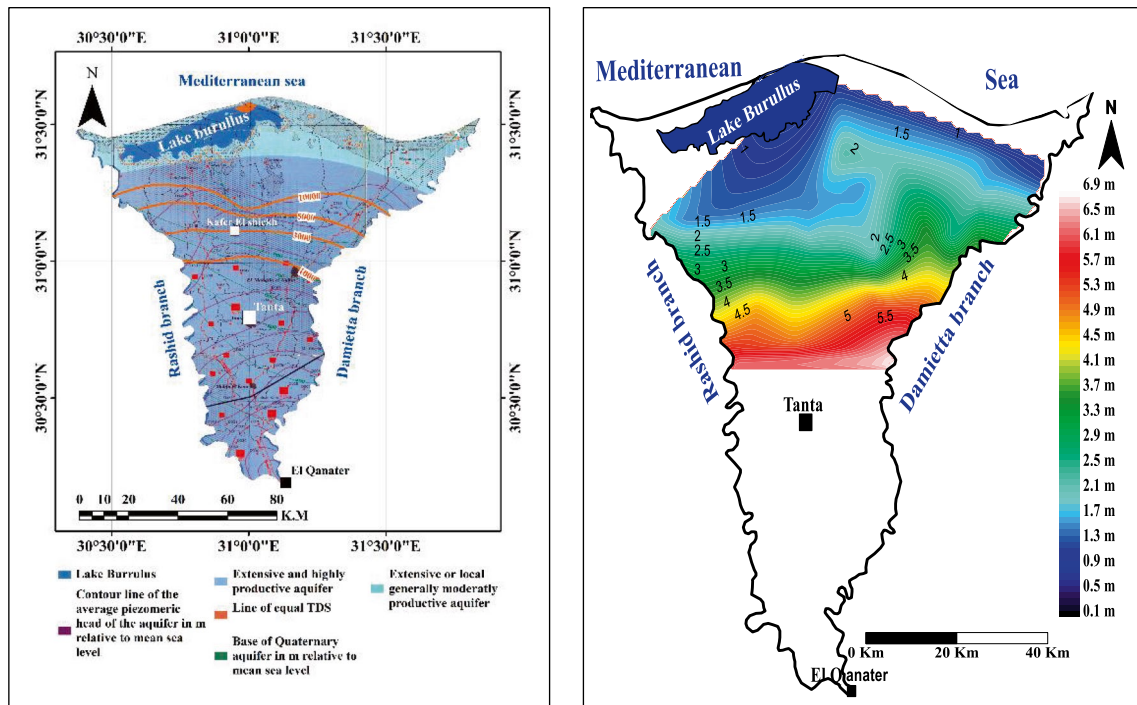
Fig. 3 A hydrogeologic map for the MND area (left panel) (RIGW 1992) and the water depths distribution map, to the north of the MND area in 1997 (right panel) (modified after Kamal 2000)

Farid (1980) reported that, the zone to the north is more saline, due to the invasion of sea water in the frontal delta, ranging from 640 to 45,000 ppm. Farid (1980) showed that, the interface, which contains gradual mixing of fresh water and salt water (transition zone), between the above fresh groundwater and the below salty groundwater, with iso-salinity lines ranging between 1000 and 35,000 ppm. Ebraheem et al. (1997) concluded that, the interface depth between the fresh and brackish water (1000–3000 ppm) increase 150 m (at Tanta city) and reduces to the north to around 40 m or less (between Qotur and Kafr El Sheikh). Also, the depth of the interface between brackish-saline zone exceeds 180 m (to the south of Kafr El Sheikh) and reduces 70 m to the northward (near village of Hadadi). FAO (2006) stated that, a noticeable the salinity of groundwater increases all over the ND region and especially at the MND (around city of Tala), which has TDS values up to 3000 ppm in 1990. The distribution of salinity in the MND part was studied by Sakr et al. (2004) and stated that, the brackish groundwater zone (2000–10,000 ppm) and saltwater (> 10,000 ppm) forms a wedge expanding into this aquifer to ~ 90 km from the coast.

Methodology

Ammar (2021) carried out a development to COMSOL numerical model to simulate the resistivity and hydroelectric characteristics of the fractured aquifers by applying DC-resistivity method (VES). He has been calibrated the analytical solutions, using the Eqs. (1 and 2) and COMSOL model. This calibration (found about < 0.03% of the percentage of error between both) was implemented for getting the best match between both for carrying out the simulation process. This Comsol model was calibrated in one layer of uniform resistivity, two layers and three layers. Equation 1 was used for computing the electric potentials (E.P.) along with a profile spanning two current electrodes (C_1C_2) in case of one layer, but Eq. 2 in case of two layers (Burger et al. 2006).

$$V_{P1} = \frac{i\rho}{2\pi}\left(\frac{1}{r_1} - \frac{1}{r_2}\right), \tag{1}$$

$$V_{P1} = \frac{i\rho_1}{2\pi r}\left[1 + 2\sum_{n=1}^{\infty} \frac{k_{1,2}^n}{\left[1 + \left(\frac{2\pi z}{r}\right)^2\right]^{\frac{1}{2}}}\right], \tag{2}$$

where V_{p1} is the potential at point 1 (V), ρ is the layer resistivity (Ω m), ρ_1 is the first layer resistivity (Ω m) above the interface, ρ_2 is the second layer resistivity (Ω m) below the interface, z is the depth (m) of interface, (I): the electric current (Ampere), r_1 & r_2 are the distance (m) from the current electrode C_1 and current electrode C_2, respectively, r is the distance (m) of the equipotential surfaces from C_1, and k is a factor depending on ρ_1 & ρ_2 ($k_{1,2} = \frac{\rho_2 - \rho_1}{\rho_2 + \rho_1}$).

Model assumptions and inputs

In this study, COMSOLs AC/DC package, COMSOL Finite Element Package, is used for simulating the effect of salinity-clay variation on the electrical potential of the aquifer along the MND. The physics in this model is electrical current and its steep or the solution is stationary, due to the assumption that, modeling the effect of salinity-clay variance on the electrical resistivity measurements is not an easy task and needs to understand how the effect of salinity and clay content on the main physical properties of the aquifer under investigation occurs. The electrical interface will be used for computing the electric field, electrical potential and electric current density distributions in the conductive medium under consideration,

with focusing on the lithologic column of the Quaternary age along the MND, that, includes the Quaternary aquifer.

In this model, the inductive effects are negligible. Depending on Ohm's law, the physics interface solves a current conservation equation, using the scalar electrical potential, as the dependent variable. The stationary study used for the field variables is constant with time. The assumed block geometry with the distribution of the occured geologic layers and their geologic, hydrogeologic and electrical (resistivity and conductivity) properties at this study are shown in Fig. 3 and reported in Tables 1, 2 and 3, as well as the location of the assumed surface cylinder, which was an interesting medium and appropriate geometric shape used for injecting the electric current through the block (one or several layers) via the two current electrodes (C_1C_2). The assumed resistivities/conductivities of the inter blocks/layers (four blocks/layers) were suggested and classified accordding to the lithology (Tables 1, 2, 3) and salinity variation into three zones. These zones were classified into fresh, brackish (transition) and saline zones, from south to north, along the MND part.

The meshes type of these layers are finer meshes, as shown in Fig. 4, right panel, while the mesh type of the surface cylinder is fine mesh (free tetrahedral mesh) (Fig. 5). The radius of this cylinder is 1.48 km and 0.02 km in its thickness and its position is 1.5 km in the X and Y and

**Table 1** Assumed model parameters for the fresh water zone of the Quaternary aquifer

Layers no.	Resistivity (Ω m)	Conductivity (S/m)	Thickness (km) equivalent to (m) in earth model	Geologic and hydrogeologic description (Schlumberger 1984, 1995; Said 1990)
L1	$\rho_1 = 150$	$\sigma_1 = 0.0066$	$h_1 = 0.08$ km (80 m)	Alternating sand and Silty clay (Quaternary Era, Holocene age) [semi-pervious layer]
L2	$\rho_2 = 4$	$\sigma_2 = 0.25$	$h_2 = 0.1$ km (100 m)	Clay [impermeable layer, aquitard]
L3	$\rho_{3-n} = 20$–40-90	$\sigma_{3-n} = 0.05$–0.025–0.011	$h_3 = 0.4$ km (400 m) Ave	Sand, gravel with clay intercalation (Quaternary Era, Pleistocene age) (Mit Ghamr Fm and El-Wastani Fm) [Main aquifer, Quaternary aquifer]
L4	$\rho_4 = 4$	$\sigma_4 = 0.25$	$h_4 = 1.4$ km (1400 m)	Clay with minor sand (Tertiary Era, Pliocene age) (Kafr El Sheikh Fm) [impermeable layer, aquiclude]

Table 2 Assumed model parameters for the brackish water zone of the Quaternary aquifer

Layers no.	Resistivity (Ω m)	Conductivity (S/m)	Thickness (km) equivalent to (m) in earth model	Geologic and hydrogeologic description (Schlumberger 1984, 1995; Said 1990)
L1	$\rho_1 = 100$	$\sigma_1 = 0.01$	$h_1 = 0.08$ km (80 m)	Alternating sand and Silty clay (Quaternary Era, Holocene age) [semi-pervious layer]
L2	$\rho_2 = 3$	$\sigma_2 = 0.333$	$h_2 = 0.1$ km (100 m)	Clay [impermeable layer, aquitard]
L3	$\rho_{3-n} = 5$–10–15	$\sigma_{3-n} = 0.2$–0.1–0.0666	$h_3 = 0.4$ km (400 m)	Sand, gravel with clay intercalation (Quaternary Era, Pleistocene age) (Mit Ghamr Fm and El-Wastani Fm) [Main aquifer, Quaternary aquifer]
L4	$\rho_4 = 3$	$\sigma_4 = 0.333$	$h_4 = 1.4$ km (1400 m)	Clay with minor sand (Tertiary Era, Pliocene age) (Kafr El Sheikh Fm) [impermeable layer, aquiclude]

**Table 3** Assumed model parameters for the saline water zone of the Quaternary aquifer

Layers no.	Resistivity (Ω m)	Conductivity (S/m)	Thickness (km) equivalent to (m) in earth model	Geologic and hydrogeologic description (Schlumberger 1984, 1995; Said 1990)
L1	$\rho_1 = 10$	$\sigma_1 = 0.1$	$h_1 = 0.08$ km (80 m)	Alternating sand and Silty clay (Quaternary Era, Holocene age) [semi-pervious layer]
L2	$\rho_2 = 0.5$	$\sigma_2 = 2$	$h_2 = 0.1$ km (100 m)	Clay [impermeable layer, aquitard]
L3	$\rho_{2-n} = 0.1$–0.5–2	$\sigma_{2-n} = 10$–2–0.5	$h_3 = 0.4$ km (400 m)	Sand, gravel with clay intercalation (Quaternary Era, Pleistocene age) (Mit Ghamr Fm and El-Wastani Fm) [Main aquifer, Quaternary aquifer]
L4	$\rho_3 = 0.5$	$\sigma_3 = 2$	$h_4 = 1.4$ km (1400 m)	Clay with minor sand (Tertiary Era, Pliocene age) (Kafr El Sheikh Fm) [impermeable layer, aquiclude]
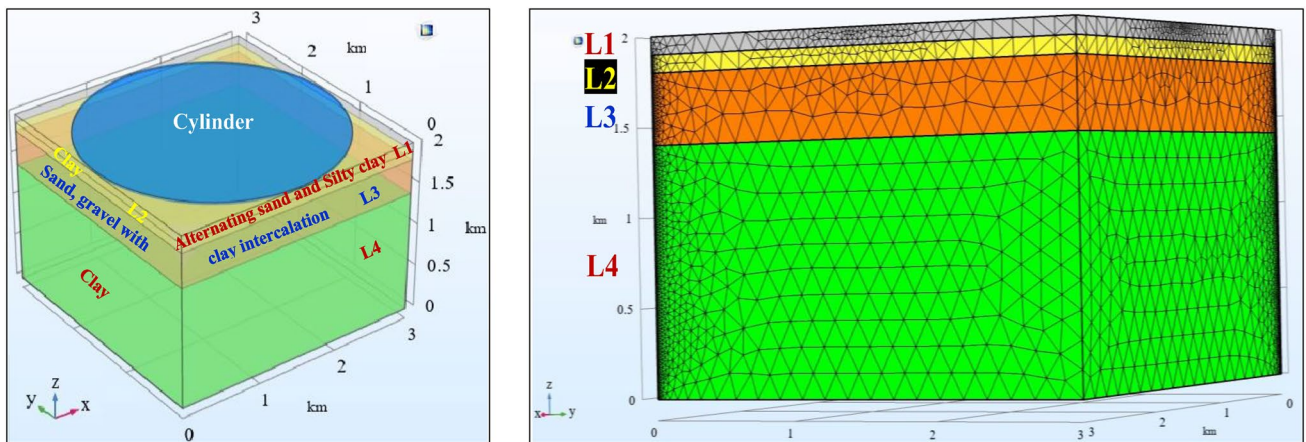
Fig. 4 A 3D view of the designed block/layers of the MND model, with the lithologic description of the subsurface geologic layers (left panel) and a 3D view of the mesh types of layers (finer mesh) (right panel)
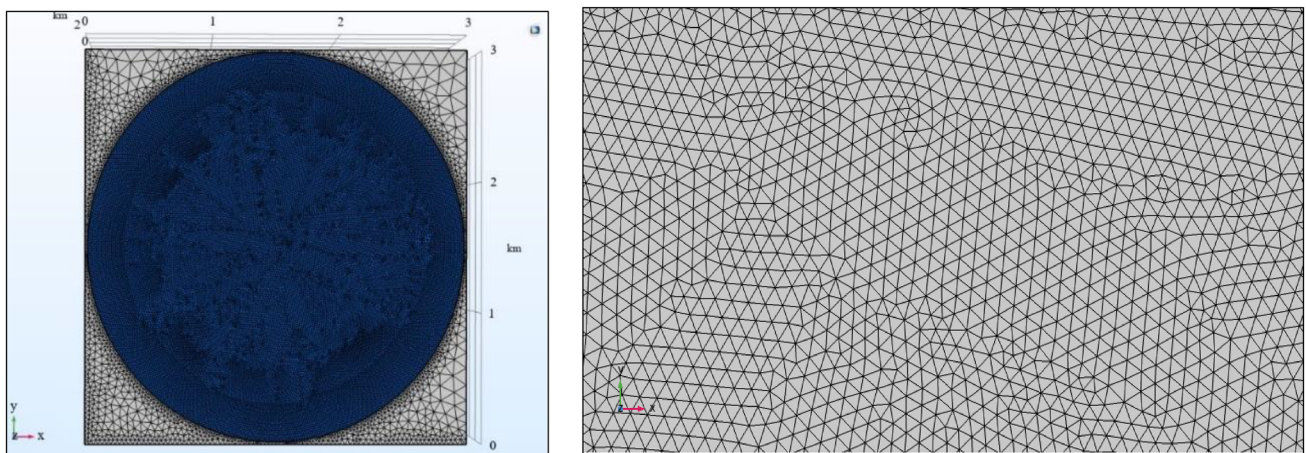
Fig. 5 The mesh types of the block in 3D view, finer mesh and surface cylinder (left panel) and fine mesh of the cylinder (right panel)

1.98 km in the Z. The resistivity of this cylinder is changed from south to north into 150 Ω m in fresh zone, to 100 Ω m in brackish zone, and to 10 Ω.m in saline zone. The first layer resistivity has the same values, as the cylinder resistivity, because it is considered a single layer or the cylinder is embedded in the surface layer (Tables 1, 2, 3). The DC current is the applied current for flow into the layers or blocks by the C_1 and C_2 electrodes of 0.05 A (50 mA).

Accordingly, the Vertical Electrical Sounding (1D VES) in this study will be used, with varying in spacings between the current electrodes (C_1 and C_2). These spacings are 0.016, 0.05, 0.08, 0.1, 0.15, 0.2, 0.3, 0.4, 0.6, 0.8, 1, 1.4, 1.8, 2 and 2.4 [km]. The model results will be included in the computed electrical potential values and curves and also calculated resistivity values and curves. Therefore, this simulation will help in understanding and solving many electrical, geologic and hydrogeological problems of the different aquifers affected by variations in salinity and clay content, with an emphasis on showing how this difference in salinity and clay volume leads to cover the main hydrogeological parameters, as well as the error in defining the type of sediment accurately.

The sea water invasion, in the Quaternary aquifer, has intruded to > 100 km from the Mediterranean Sea coast (Sakr 2005). The groundwater fresh zone began to discharge from the south of Tanta city till the south of Kafr El Sheikh city. Therefore, we have chosen the first three VESes (VES1, VES2, and VES3) from 10 km South Tanta city to 20 km North Tanta city where the fresh zone occurs. The groundwater of northern Kafr El Sheikh city is highly affected by saltwater invasion. Therefore, we have chosen the VESes 7, 8 and 9 to the north of Kafr El Sheikh city and South Lake Burullus where the saline zone lies. The groundwater especially at the shallow depths is highly affected by sea water invasion (TDS ~ 2000 ppm), and the groundwater especially the deeper depths is of hypersaline (80,000 ppm) (Negm 2019). The area located between the two zones, from near south to near north of Kafr El Sheikh city, was chosen as a transition zone and the VESes 4, 5, and 6 were existed through this zone. Based on Sakr et al. (2004), we chosen a distance of 80 km to study the effect of salinity-clay variation on the electrical potential of the Quaternary aquifer from 10 km south of Tanta city to the southern edge of Lake Burullus.

According to the previous data, the selected area was classified into three groundwater zones, the fresh groundwater zone, the transition groundwater zone and the saline groundwater zone. The model will have four layers, as reported in Fig. 4, left panel, and Tables 1, 2 and 3. 1st layer is alternating sand and silty clay. 2nd layer is clay [impermeable layer, aquitard]. 3rd layer is sand and gravel with clay intercalations (Pleistocene age) (Mit Ghamr Fm and El-Wastani Fm) [Main aquifer of Quaternary age]. 4th layer is clay, with minor sand (Pliocene age) (Kafr El Sheikh Fm) [impermeable layer, aquiclude]. Depending on the previous depths to the groundwater, a high resistivity value is chosen to the first layer (L1) in the southern parts (south to the

near north of Tanta city of fresh zone), medium resistivity value to this layer in the central parts of the Nile Delta, especially in the near south to the near north of Kafr El Sheikh city (transition zone) and low resistivity value to the first layer (L1) to the northern parts of the ND especially to the near north of kafr El Sheikh to the south of Burullus Lake, as reported in Tables 1, 2 and 3. Also, according to the groundwater salinity values of this aquifer (L3) and the clay content, as shown in the hydrogeological map (Fig. 3, left panel), as mentioned in the previous explanation and also as shown in Fig. 2, the resistivity values for this aquifer were selected, as reported in Tables 1, 2 and 3, as well as the clay layer (L2) at the base of the Holocene deposits and the Pliocene (L4) clay layer at the base of this aquifer.

Table 1 describes the assumed parameters of the simulation of the four layers, using COMSOL Multiphysics model at the fresh zone. These parameters include the ranges of resistivity (Ω m), conductivity (S/m) (Ebraheem et al. 1997 and Attwa et al. 2014) and thickness (m), in addition to the geologic and hydrogeologic description of the four geologic layers at the fresh zone. The TDS of the Quaternary aquifer in this zone is ≤ 1000 ppm. This zone extends from south of Tanta city to the near north of the same city.

Table 2 exhibits the assumed parameters of the simulation for the four layers, using COMSOL Multiphysics model at the brackish (transition) zone. These parameters include the ranges of resistivity, conductivity (Ebraheem et al. 1997) and thickness, in addition to the geologic and hydrogeologic description of the geologic layers at the brackish zone. The salinity of the Quaternary aquifer is slight to moderate and its TDS is 1000–10,000 ppm. This zone extends from the near south to the near north of Kafr El Sheikh city.

Table 3 reveals the assumed parameters of the simulation for the four layers using COMSOL Multiphysics model at the saline zone, due to sea water intrusion. These parameters include the ranges of resistivity, conductivity (Ebraheem et al. 1997 and Ammar et al. 2021) and thickness, in addition to the geologic and hydrogeological description of the geologic layers at the high saline zone. Kumar et al. (2021) stated that the ERT survey showed low resistive zones (0–5 Ωm) as an indicator of seawater intrusion. The groundwater of the Quaternary aquifer is highly saline water and its TDS is > 10,000 ppm. This zone extends from far north of Kafr El Sheikh city till the area of Burullus Lake to the near south of the lake. According to RIGW (1992), Salem et al. (2008) and other authors, the clay content and clay lenses, and their thicknesses increase toward the northern direction.

Governing equations

Equation 3 is the assuming equation in case of electric current:

$$\nabla \cdot J = Q_{j \bullet v}, \tag{3}$$

where $Q_{j•v}$ is a volumetric source of current inside the selected layers (A/m^3) and J is the density of current (volume) (A/m^2).

A discretization and dependent variable are the electrical potential V2. The relation defines that; the current density is circulated by introducing a current. This current generated externally (Je). The resulting constitutive relations are shown as follow:

$$J = \sigma E, \qquad (4)$$

$$J = \sigma E + J_e, \qquad (5)$$

$$E = -\nabla v, \qquad (6)$$

where σ is the electrical conductivity (EC) (S/m), E is the electrical field, v is the electrical potential (V), and Je is the external current density (A/m^2).

## Model outputs

Model outputs in case of fresh water zone

Electrical potential and current density description

For each of the three cases of water salinity zones; whether in fresh, brackish or salt-water areas, VES technique has been used, to calculate the electrical potential in both current electrodes of the electric current (C_1 and C_2), with changing the spacings between them. This potential is due to the flow of electric current through the subsurface layers/blocks. As the electric current flows through these layers of different resistivities, the density of this current will vary, depending on whether the layers are either resistive or conductive. Therefore, when the layer is resistive, the current density

will be low, while in case of the conductive layer, the current density will be high. In this case, the suggested resistivities of the existing layers are high, low and medium to high and low. Thus, the higher current density is expected to be present at the layers with lower resistivity values. Figure 6 in 3D view and $X–Y$ view show the resultant electric potential; as multiple slices, slices (rainbow color) and contours (yellow color), as well as the electrical current density as streamlines (magenta color) for the case of VES1 in the zone of fresh water, when the spacings between C_1 and C_2 is 1000 m ($C_1C_2/2 = 500$ m). Figure 7 is in the $X–Z$ view, to show the current density, with it focusing in each layer and with depth, in the form of streamlines (magenta color).
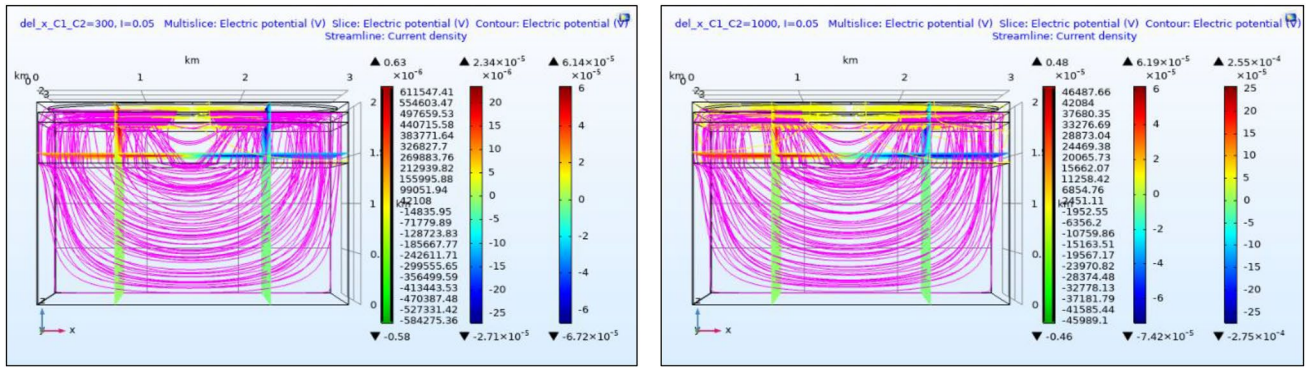
In this case, the electrical potential contours at both electrodes of the current appear, as symmetrical contour lines. This short distance between the current electrodes (1000 m) shows the values of electrical potential and current density at shallow depths, where the L1 and L2 layers are existing. Also, in this case, where the spacing between the electrodes is 1000 m, then the electrical potential values are expressed and the electric current density are exhibited at the far depths, where the Quaternary aquifer layer (L3) occurs, as shown in Fig. 6, in the case of VES1. Also, Fig. 7 reveals the electrical potential in the XZ view, with focusing on the current density (magenta streamlines) in the XZ view, in the case of 300 m and 1000 m electrode spacings. It was found that, the electric current density is high at the shallow depths, in the case of 300 m spacing, while it is high in the far depths, when the spacing is 1000 m.

Therefore, it can be concluded that, the electric current will be concentrated at shallow depths, when the distances between the electrodes are small. While this current is more concentrated in the deep depths, in the case of large electrode spacing because the electric current passes quickly at shallow depths and will penetrate deeper to the far depths.
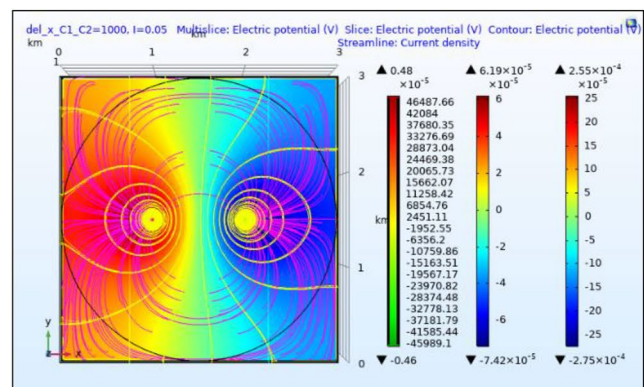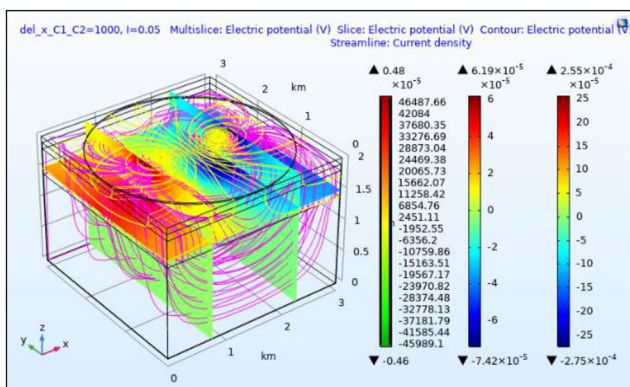
Fig. 6 The electrical potential values in 3D view in multislices, slices (rainbow color) and contours (yellow color), as well as the current density in streamlines (magenta color) (volume) (left panel) and a $X–$ Y view (right panel) of VES1 when the spacings between C_1 and C_2 is 1000 m, in case of fresh zone
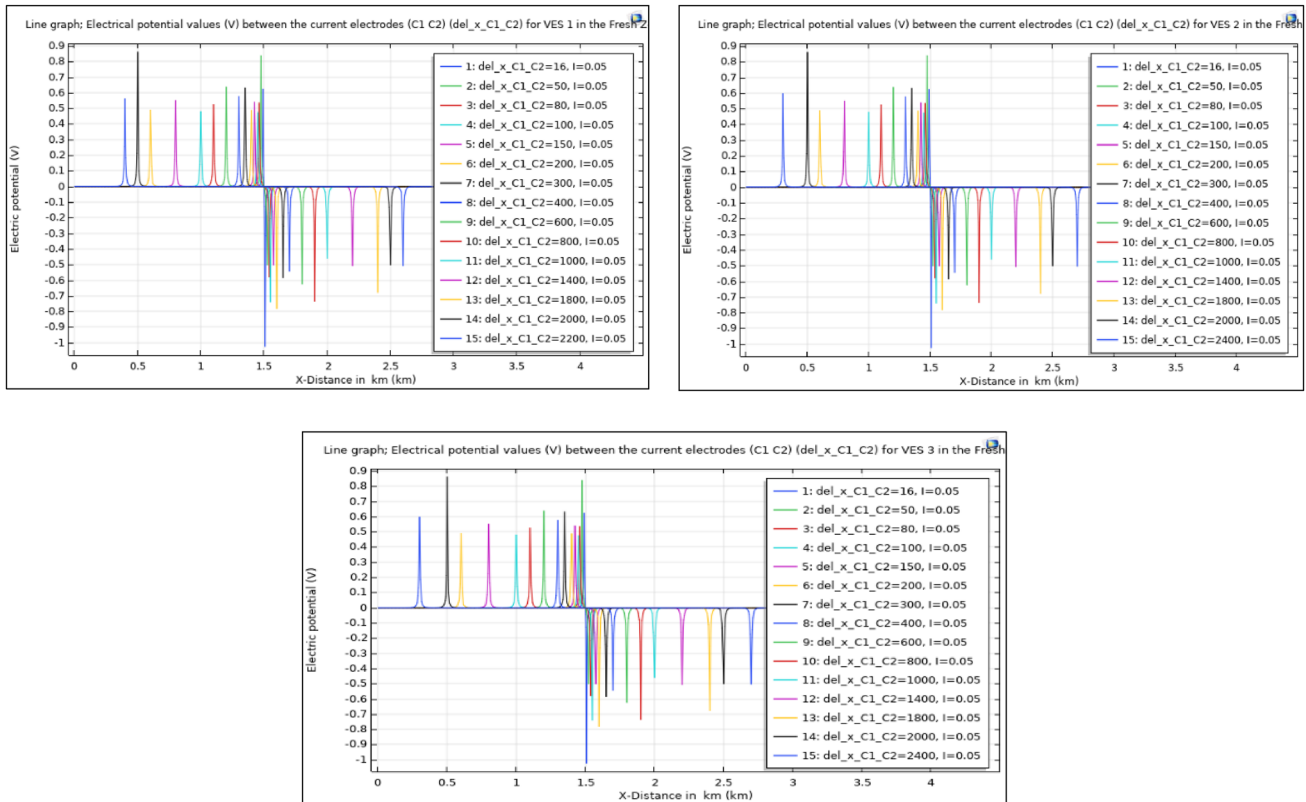
Fig. 7 A *XZ* view of the electrical potential values in multislices, slices, (rainbow color) and contours (yellow color), with focusing on the current density in streamlines (magenta color) of VES1, when the spacings between C_1 electrode and C_2 electrode are 300 m (left panel) and 1000 m (right panel), in case of fresh groundwater zone

This current takes a semi-circular shape, especially at shallow or far depths and this shape is more obvious, in the case of thick layers (Fig. 7). Accordingly, the electric potential values of the Quaternary aquifer are high, in the case of fresh zone. Whereas, the density of current in this aquifer is low to medium, due to its high values of resistivity and the occurrence of fresh groundwater, as well as the low clay content, which are major factors in reducing the values of resistivity of the materials.

Fig. 8 The electrical potential values between the electrodes of VES1 (upper left panel), VES2 (upper right panel), and VES3 (lower panel), when the resistivities of aquifer are 90, 40 and 20 Ω m, respectively, in case of fresh zone

Table 4 The electrical potential values and the apparent resistivity values of the fresh zone (VESes 1, 2 and 3), with the subsurface lithologic description

C1C2l2 in m	Electrical Potential values (V) of VES1 when aquifer resistivity is 90 Ω m	App. Resistivity values (Ω m) of VES1 when aquifer resistivity is 90 Ω m	Electrical Potential values (V) of VES2 when aquifer resistivity is 40 Ω m	App. Resistivity values (Ω m) of VES2 when aquifer resistivity is 40 Ω m	Electrical Potential values (V) of VES3 when aquifer resistivity is 20 Ω m (low clay)	App. Resistivity values (Ω m) of VES3 when aquifer resistivity is 20 Ω m (low clay)	Lithology
8	0.146901943	174	0.146901943	174	0.146901943	174	Surface layer
25	0.019064522	121	0.019064522	121	0.019064522	121	
40	0.002377464	69	0.002377464	69	0.002377464	69	
50	0.001042652	45	0.001042803	45	0.001042803	45	
75	0.00012176	14	0.000122222	14	0.000122222	14	Clay
100	4.00339E−05	7	3.99139E−05	7	3.99139E−05	7	
150	1.10136E−05	5	1.08477E−05	5	1.08477E−05	4.7	
200	8.85444E−06	6	8.58657E−06	5.5	8.24804E−06	5	Quaternary aquifer
300	4.68614E−06	10	4.39039E−06	8.5	4.03087E−06	7.8	
400	9.0491E−06	21.5	6.99123E−06	15.5	6.55702E−06	14.8	
500	1.34485E−05	38	1.07112E−05	30	9.25053E−06	26	
700	1.3899E−05	77.5	8.59583E−06	43	9.20172E−06	36.5	
900	1.69609E−05	90	1.2407E−05	49	1.1519E−05	38	
1000	1.82343E−05	83	1.11309E−05	43	1.25831E−05	36	
1200	2.02917E−05	64	1.73653E−05	35	1.47027E−05	28.5	

Calculation of the electrical potential and apparent resistivity of the fresh water zone

To calculate the electrical potential values in each layer with successive depths in this zone, three VESes were performed, assuming the aquifer resistivities are 90, 40 and 20 Ω m. After obtaining the electrical potential values between the electrodes (C_1 and C_2), with the change of the spacing between them for each VES, as shown in Fig. 8, the apparent resistivity was calculated using Eq. 7 for each $C_1C_2/2$, as in Table 4. The calculation of this resistivity shows that, the electrical potential of the aquifer decreases with decreasing the resistivity values, due to the increase in water salinity and clay content. In this case, the decrease was found to be slight because the salinity of this aquifer is less than 1000 ppm and the clay content is low ($< 10\%$), as mentioned in the previous hydrogeologic conditions of the aquifer in this zone. For an array of current electrodes, as the used Schlumberger array in this study, C_1 and C_2 (the current electrodes 1 and 2), and P_1 and P_2 (the potential electrodes 1 and 2), the resistivity (Ω m) is calculated by the following Eq. 7:

$$\rho_a = \frac{2\pi}{\frac{1}{C_1P_1} - \frac{1}{C_2P_1} - \frac{1}{C_1P_2} + \frac{1}{C_2P_2}} \frac{\Delta V}{I}, \quad (7)$$

where ρ_a is the apparent resistivity (Ω m), I is the current intensity (Ampere) and ΔV is the potential difference between the potential electrodes (V)
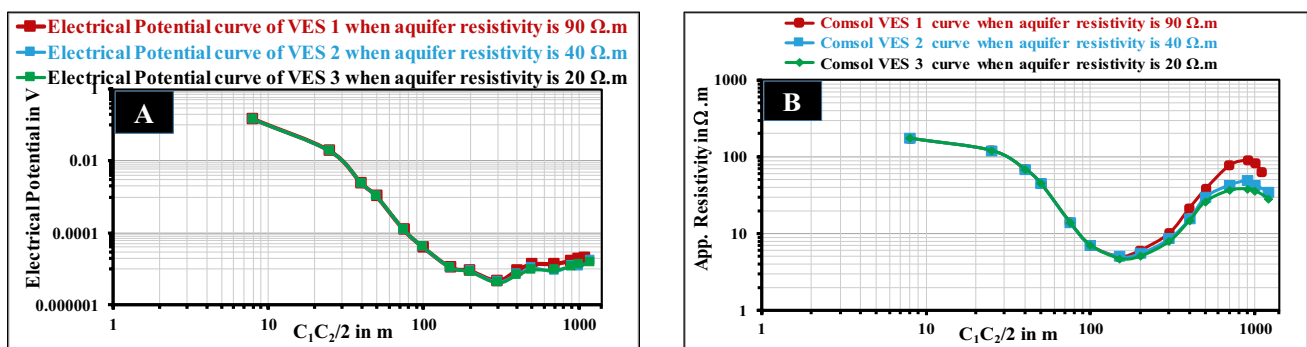
In case of aquifer resistivity is 90 Ω m (VES1)

After calculating the electrical potential at the center of each two current electrodes ($C_1C_2/2$), with changing the distance between them (Fig. 8, upper left panel), and when the groundwater aquifer resistivity was 90 Ω m, the VES1 electrical potential curve was resulted (Fig. 9A). The apparent

resistivity curve was also produced, as exhibited in Fig. 9B, by calculating the apparent resistivity (ρ_a), using Eq. 7. The apparent resistivity curve shows that, these apparent resistivities change with depth, depending on the characteristics of the layers (Table 4) (Fig. 9B). In this case, the minimum electrical potential value (4.68614E−06V) was recorded for the Quaternary aquifer when $C_1C_2/2 = 300$ m after the electric current penetrated the upper clay layer. While the maximum value (2.02917E−05V) was recorded, when the $C_1C_2/2 = 1200$ m, after the electric current passed through the aquifer layer, especially at the lower depths of the aquifer before reaching the upper depths of the last layer (L4). It was also noted that, the lower values of the apparent resistivity decrease, due to the effect of high conductivity of the clay layer, which is located below the Quaternary reservoir (L4), as shown in Table 4 and Fig. 9B.

The higher calculated value of the apparent resistivity of the aquifer was 6 Ω m, as a result of the high effect of the upper conductive clay layer (L2) and due to the absorption of electric current during passing through the interface between them. While this effect is low, when the lower value of the apparent resistivity of this aquifer was 64 Ω m, due to the current penetration at the shallow parts of the interface between the layers: L3 (aquifer) and L4 (clay). This is indicated that, when there are high conductive or very low resistive layers, such as L2 (clay) over high resistive layers, they will reduce the resistivity of the high resistive substrata layers, especially at the higher depths.

In case of aquifer resistivity is 40 Ω m (VES2)

From the calculation of the electrical potential between each of the two different electrodes in VES2, as shown in Fig. 8, upper right panel, when the assumed resistivity value of the aquifer is 40 Ω m, the values of the electrical potential, in the middle parts of the electrodes, were determined, with the difference of $C_1C_2/2$, as shown in Table 4 and Fig. 9A. It is also resulted in calculating the apparent resistivity values at

Fig. 9 The electrical potential curves (**A**) and the apparent resistivity curves (**B**) of VESes 1, 2 and 3, when aquifer resistivities are 90, 40 and 20 Ω m, in case of fresh zone

each $C_1C_2/2$ and then the VES2 curve, representing the fresh zone, as shown in Table 4 and Fig. 9B. From Table 4, and from the electrical potential and apparent resistivity curve, of VES2 (Fig. 9), the minimum and maximum electrical potential values of the aquifer are (4.39039E−06V) and (1.73653E−05V), when the spacings between the electrodes ($C_1C_2/2$) are 300 m and 1200 m, respectively. While the calculated minimum and maximum apparent resistivity values are 5.5 Ω m and 49 Ω m, respectively. It was noted from this configuration that, the electrical potential and apparent resistivity values, in this case (VES2), are slightly lower than the values in case of VES1.

In case of aquifer resistivity is 20 Ω m (VES3)

Also, after calculating the electrical potential (VES3) between the current electrodes ($C_1C_2/2$) (Fig. 8, lower panel), in case of the assumed groundwater aquifer resistivity is 20 Ω m, the electrical potential values were determined at the middle of the different distances between the electrodes ($C_1C_2/2$) (Table 4 and Fig. 9A). Also, the ρ_a values of VES3 were calculated at each $C_1C_2/2$, resulting in an ρ_a curve (Fig. 9B). It was found that, the minimum and maximum electrical potential values of the aquifer are (4.03087E−06V) and (1.47027E−05V), respectively. While the apparent resistivity values are 5 and 38 Ω m, when the electrode spacings $C_1C_2/2$ are 200 m and 900 m, respectively (Table 4 and Fig. 9B). The previous values indicate a slight decrease in these values of this VES3, as compared to the case of VES2, and there is a moderate decrease from VES1 due to the increase in clay content.

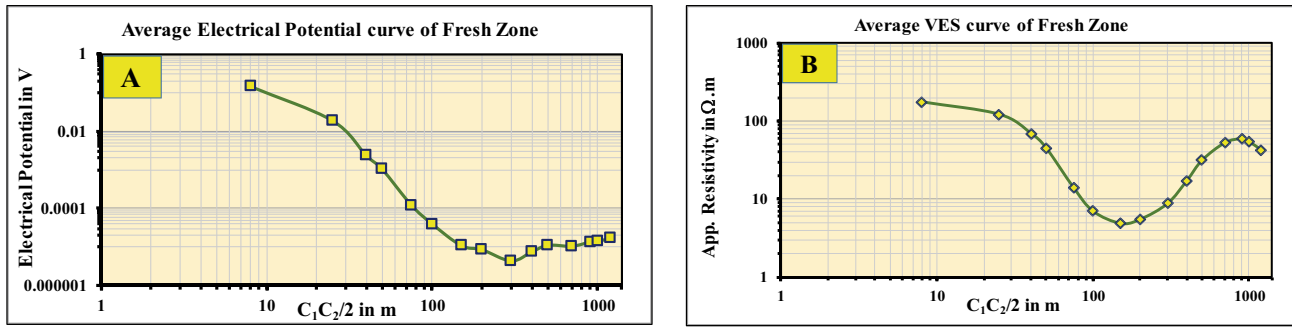### Comparison between the electrical potential and apparent resistivity of the fresh zone

From the comparison between the calculated electrical potential values and the calculated apparent resistivity values of the VESes (VES1, VES2 and VES3), for the fresh zone of the Quaternary aquifer, as shown in Table 4 and Fig. 9, there is a slight decrease in the apparent resistivity values of the aquifer, when the spacings between current electrode vary from 200 to 1200 m. This slight difference indicates that, the electrical potential of the aquifer in the fresh zone condition is little affected by the decrease in salinity and clay content. This case reflects that, the fresh water with lower clay content has less influence on the electrical potential and resistivity values of the aquifer. Therefore, the electrical potential and ρ_a values are high in the case of fresh water and little clay content, where this helps in the prediction and evaluation of the salinity and clay content. Accordingly, it can be indicated that, the previous three curves of the VESes indicate that, the aquifer that, was explored contains fresh water with clean sediments, as well as containing low clay content and that, the maximum ranges of the apparent resistivity values are 90, 49 and 38 Ω m, as recorded at the middle depths of the examined aquifer.

Average values of the electrical potential and apparent resistivity of the fresh zone sediments

Depending on the calculation of the electrical potential values and the ρ_a values in the three cases of the VESes of the fresh zone, the average electrical potential values and the average apparent resistivity values of the Quaternary aquifer in the fresh

Table 5 The average electrical potential values and the apparent resistivity values of the fresh zone, with the subsurface lithologic description

$C_1C_2/2$ in m	Average electrical potential values (V) in fresh zone	Average App. resistivity values (Ω m) in fresh zone	Lithology
8	0.146901943	174	Surface layer
25	0.019064522	121	
40	0.002377464	69	
50	0.001042753	45	
75	0.000122068	14	Clay
100	3.99539E−05	7	
150	1.0903E−05	5	
200	8.56301E−06	6	Quaternary aquifer
300	4.36914E−06	9	
400	7.53245E−06	17	
500	1.11367E−05	31	
700	1.05655E−05	52	
900	1.36289E−05	59	
1000	1.39827E−05	54	
1200	1.74532E−05	43	

Fig. 10 The average electrical potential curve (**A**) and the average apparent resistivity curve (**B**) of VESes in case of fresh zone

zone (Table 5), were found that, the minimum and maximum values of the electrical potential of the concerned aquifer are (4.36914E–06 V) and (1.74532E–05 V), respectively. The minimum and maximum values of the apparent resistivities were 6 Ω m, due to the influence of the upper clay, and 59 Ω m, respectively. These results also led to the determination of the average curve of the electrical potential curve and the ρ_a of the layers of Quaternary in the fresh zone along the MND, especially from the north of the city of Tanta, near to the south, as shown in Fig. 10. These two curves can be generalized to the Quaternary sediments along the Nile Valley, especially from Tanta city, also to the southeast and southwest of the Delta, where the fresh zones of the Quaternary aquifer are located.

Model outputs in case of brackish water zone

In this case of VES6 in the brackish zone, the electrical potential values are illustrated and the electric current density are represented at the far depths, where the Quaternary aquifer layer (L3) occurs. Figure 11 shows the electrical potential in *XZ* view with focusing on the current density in *XZ*

view, when the spacings between C_1 and C_2 are 300 m and 1000 m. From these figures, the electric current density is high at shallow depths, while it is very high at the far depths when the spacing is 1000 m. Therefore, the electric current will be concentrated at shallow depths, while this current is more concentrated at the deep depths, in the case of large electrodes spacings. This is due to that, the electric current passes quickly at shallow depths and penetrate deeper to the far depths. Accordingly, the electric potential values of the Quaternary aquifer are high in the case of brackish zone, whereas the current density in this aquifer is low to medium, due to its high resistivity value, and the presence of brackish water and medium clay content.

Calculation of the electrical potential and apparent resistivity of the brackish water zone

To compute the electrical potential values of the assumed four layers, three VESes were carried out, assuming the resistivities of the aquifer are 15, 10 and 5 Ω m. After getting the electrical potential values between the electrodes
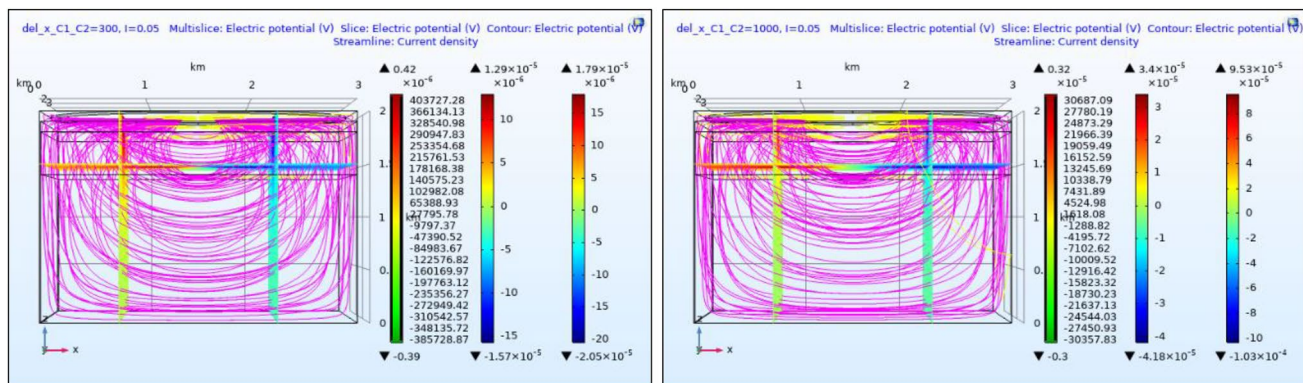
Fig. 11 A *XZ* view of the electrical potential values in multislices, slices, (rainbow color) and contours (yellow color), with focusing on the current density in streamlines (magenta color) of VES6, when

spacings between C_1 and C_2 are 300 m (left panel) and 1000 m (right panel), in case of brackish water zone
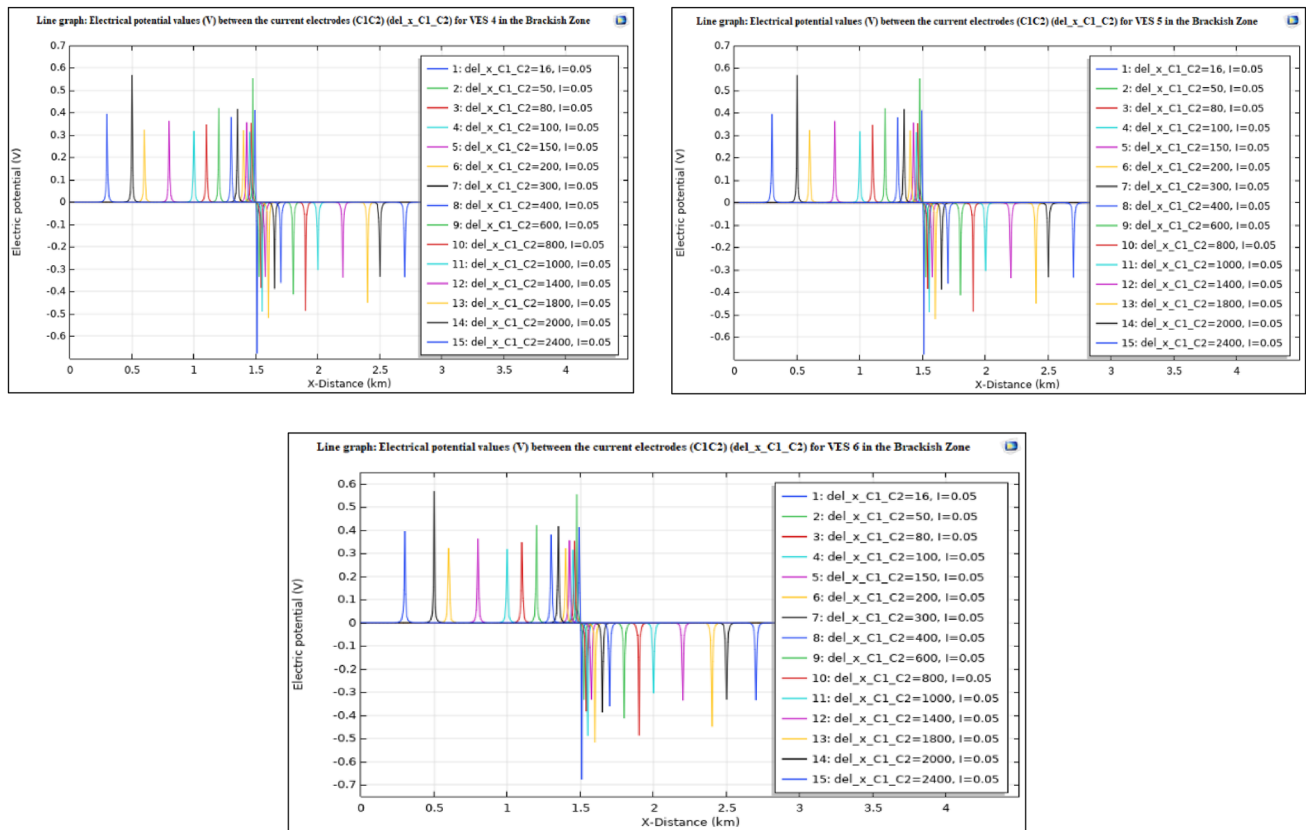
Fig. 12 The electrical potential values between the electrodes of VES4 (upper left panel), VES5 (upper right panel), and VES6 (lower panel), when the aquifer resistivities are 15, 10 and 5 Ω m, respectively, in case of brackish zone

$(C_1$ and $C_2)$ (Fig. 12) for each VES, the apparent resistivity was calculated, as in Table 6. The calculation of this resistivity shows that, the electrical potential of the aquifer decreases with decreasing the resistivity values, due to the slight increase in water salinity and clay content. Therefore, the decrease was found to be slight, because the salinity is > 1000 and < 10,000 ppm, and the clay content is low to medium as mentioned in the previous hydrogeologic conditions of the aquifer in this zone.

In case of aquifer resistivity is 15 Ω m (VES4)

After computing the electrical potential at the center of each two current electrodes $(C_1C_2/2)$ (Fig. 12, upper left panel), when the groundwater aquifer resistivity was 15 Ω m, the electrical potential curve of VES4 was resulted (Fig. 13A). The apparent resistivity curve was also produced, as in Fig. 13B and shows that, the apparent resistivities change with depth, depending on the characteristics of the layers (Table 6) (Fig. 13B). The minimum electrical potential value of the Quaternary aquifer in this case is 2.35796E–06 V, when the electrodes spacing was

600 m $(C_1C_2/2 = 300$ m). While the maximum value is 1.10187E–05 V, when the spacing between the electrodes was 2400 m $(C_1C_2/2 = 1200$ m). It was also noted that, the last value of the apparent resistivity decreases, due to the effect of high conductivity of the clay layer, as well as the salinity effect (Table 4 and Fig. 9B).

In case of aquifer resistivity is 10 Ω m (VES5)

The higher calculated value of the apparent resistivity of the aquifer was 3.7 Ω m, as a result of the highly conductive clay bed effect (L2), due to the absorption of electric current and to effect of salinity and clay content, where this effect is high. While this effect is medium, when the lower value of the resistivity of this aquifer was 34 Ω m, due to the current penetration at the shallow parts of the interface between the layers L3 (aquifer) and L4 (clay). This confirms that, when there are high conductive or very low resistive layers, such as L2 (clay) over medium resistive layers, they will reduce the resistivity of the medium resistive substrate layers especially at the higher depths of the substrate.

From the calculation of the electrical potential between the electrodes in VES5, as shown in Fig. 12, upper right panel, the

Table 6 The electrical potential values and the apparent resistivity values of the brackish zone (VESes 4, 5, and 6), with the subsurface lithologic description

$C_1C_2/2$ in m	Electrical Potential values (V) of VES4 when aquifer resistivity is 15 Ω m (medium Clay with Brackish water)	App. Resistivity values (Ω m) of VES4 when aquifer resistivity is 15 Ω m (medium Clay with Brackish water)	Electrical Potential values(V) of VES5 when aquifer resistivity is 10 Ω m (medium Clay with Brackish water)	App. Resistivity values (Ω m) of VES5 when aquifer resistivity is 10 Ω m (medium Clay with Brackish water)	Electrical Potential values (V) of VES6 when aquifer resistivity is 5 Ω m (high Clay with Brackish water)	App. Resistivity values (Ω m) of VES6 when aquifer resistivity is 5 Ω m (high Clay with Brackish water)	Lithology
8	0.096961783	114	0.096961783	114	0.096961783	114	Surface layer
25	0.012604861	80	0.012604861	80	0.012604861	80	
40	0.001581079	46	0.001581079	46	0.001581079	46	
50	0.000697632	30	0.000697632	30	0.000697632	30	
75	8.45968E−05	10	8.45968E−05	10	8.45968E−05	10	Clay
100	2.87042E−05	4.8	2.87042E−05	4.8	2.87042E−05	4.8	
150	7.97051E−06	3.5	7.97051E−06	3.5	7.97051E−06	3.5	
200	6.19101E−06	3.7	6.00684E−06	3.6	6.67483E−06	3.4	Quaternary aquifer
300	3.02616E−06	5.9	2.83359E−06	5.6	3.27104E−06	5.7	
400	2.35796E−06	10.5	4.44635E−06	10.3	2.52139E−06	10	
500	4.03497E−06	17	3.92899E−06	16.4	3.75041E−06	15.5	
700	6.50409E−06	43	6.12863E−06	32	5.59243E−06	29	
900	8.20716E−06	44	8.26404E−06	39	7.18461E−06	34.5	
1000	8.86913E−06	40	8.84073E−06	38	8.45951E−06	35	
1200	1.10187E−05	34	1.01017E−05	28.5	9.49664E−06	24	
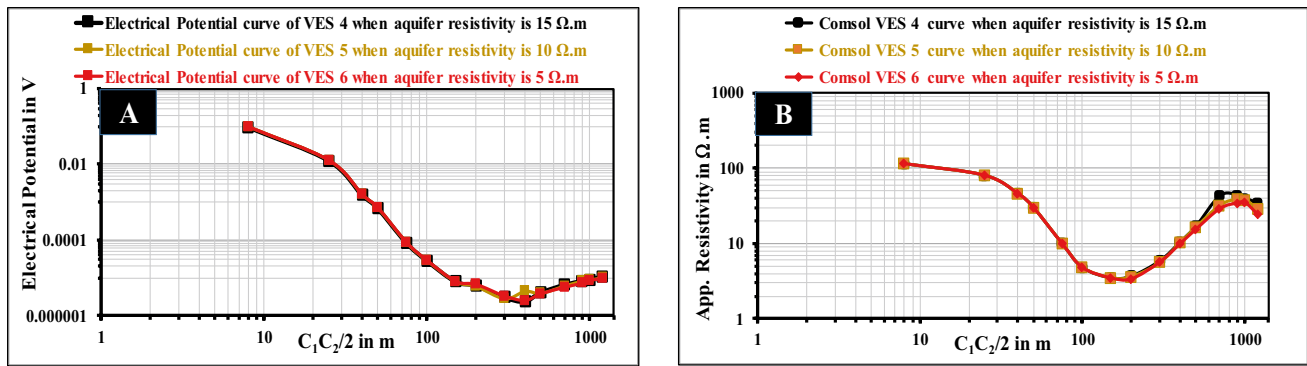
Fig. 13 The electrical potential curves (**A**) and the apparent resistivity curves (**B**) of VESes 4, 5 and 6, when the aquifer resistivities are 15, 10, and 5 Ω m, in case of brackish zone

values of the electrical potential were determined with the difference of $C_1C_2/2$ (Table 6 and Fig. 13A). It is also resulted in calculating the apparent resistivity values at each $C_1C_2/2$ and then the VES5 curve represent the brackish zone (Table 6 and Fig. 13B). From Table 6, and from the electrical potential and apparent resistivity curves of VES5 (Fig. 13), the minimum and maximum values of electrical potential of the aquifer are (2.83359E–06 V) and (1.01017E–05 V), when $C_1C_2/2$ are 300 m and 1200 m, respectively. The minimum and maximum apparent resistivity values are 3.6 Ω m and 39 Ω m, respectively. It was noted that, the electrical potential and apparent resistivity values in this case (VES5) are slightly lower than the values in the case of VES5.

In case of aquifer resistivity is 5 Ω m (VES6)

After computing the electrical potential between the current electrodes of VES6 (Fig. 12, lower panel), see Table 6 and Fig. 13A, the apparent resistivity values of this VES were calculated at each $C_1C_2/2$, resulting in an apparent resistivity curve, as shown in Fig. 13B. The minimum and maximum electrical potential values of the aquifer are (2.52139E–06 V) and (9.49664E–06 V), respectively. While the minimum and maximum apparent resistivity values are 3.4 and 35 Ω m, when $C_1C_2/2$ is 200 m and 1000 m, respectively (Table 6 and Fig. 13B). The previous values indicate also a slight decrease in the electrical potential and apparent resistivity values of VES6, compared to the case of VES5, and there is a moderate decrease from the case of VES4, due to the presence of low to medium clay content in this zone.

Comparison between the electrical potential and apparent resistivity of the brackish zone

From the comparison between the computed electrical potential values and the calculated apparent resistivity
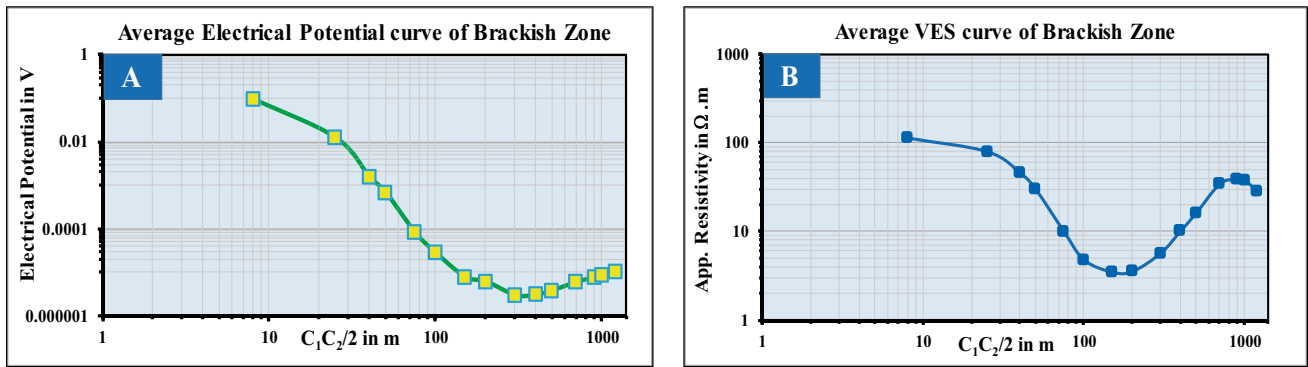
values of the VESes (VES4, VES5 and VES6) for the brackish zone of the Quaternary aquifer, as shown in Table 6 and Fig. 13, there is a medium decrease in the electrical potential and apparent resistivity values of the aquifer when $C_1C_2/2$ is varied from 200 to 1200 m. This medium decreasing indicates that, the electrical potential of the aquifer in this zone is medium, as affected by the decrease in salinity and clay content. This case reflects that, the brackish water with medium clay content has less influence on the electrical potential and the aquifer ρ_a values. Therefore, the electrical potential and ρ_a values are medium in the case of brackish water and medium clay content. These values are reduced clearly in the case of increase in clay content with the presence of brackish zone (of VES6). This helps in the prediction and evaluation of salinity and clay content. Accordingly, the maximum ranges of the apparent resistivity values are 44, 39 and 35 Ω m, as recorded at the middle depths of the aquifer.

Average values of the electrical potential and apparent resistivity of the brackish zone sediments

Depnding on the computation of the electrical potential values and the ρ_a values in the three previous cases of the VESes of the brackish zone, the average of these values of the Quaternary aquifer in this zone (Table 7), were found that, the expected minimum and maximum values of the electrical potential of this aquifer are (3.0436E−06 V) and (1.02057E−05 V), respectively. While the calculated values of the apparent resistivity were 3.6 Ω m, due to the influence of the upper clay, and 39.2 Ω m, respectively, and also to the presence of medium to high clay content, with brackish water in the aquifer. These results also led to the determination of the average electrical potential curve and the apparent resistivity curve of the layers of Quaternary in the brackish zone along the MND, especially from the far north of

Table 7 The average electrical potential values and the apparent resistivity values of the VESes at the brackish zone, with the subsurface lithologic description

$C_1C_2/2$ in m	Average electrical potential values (V) in brackish zone	Average App. resistivity values (Ω m) in brackish zone	Lithology
8	0.096961783	114	Surface layer
25	0.012604861	80	
40	0.001581079	46	
50	0.000697632	30	
75	8.45968E−05	10	Clay
100	2.87042E−05	4.8	
150	7.97051E−06	3.5	
200	6.29089E−06	3.6	Quaternary aquifer
300	3.0436E−06	5.7	
400	3.10857E−06	10.3	
500	3.90479E−06	16.3	
700	6.07505E−06	34.7	
900	7.88527E−06	39.2	
1000	8.72312E−06	37.7	
1200	1.02057E−05	28.8	

Fig. 14 Average electrical potential curve (**A**) and average the apparent resistivity curve (**B**) of the VESes, in case of brackish zone
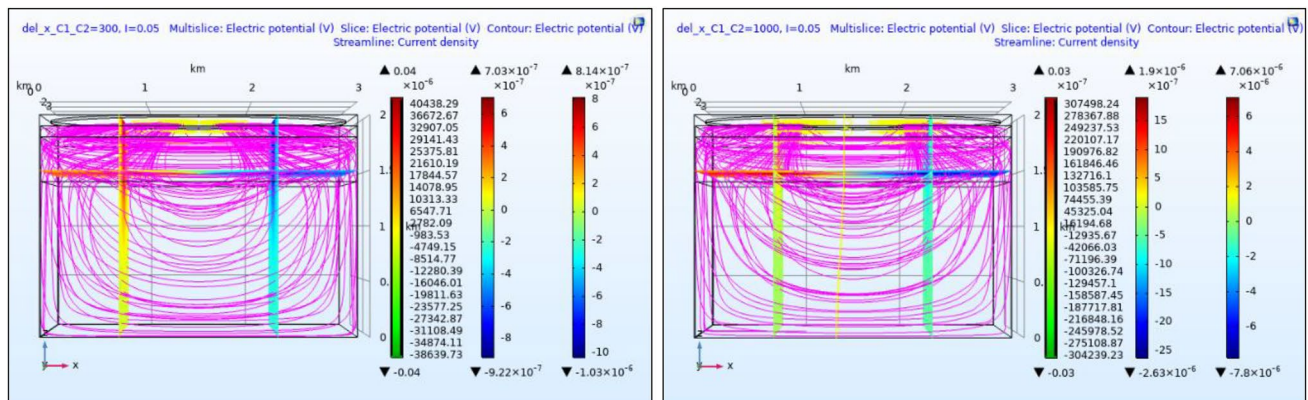
Fig. 15 The electrical potential (*V*) values in *XZ* view in multislices, slices, (rainbow color) and contours (yellow color), with focusing on the current density in streamlines (magenta color) of VES9, when the spacings between *C*1 and *C*2 are 300 m (in left panel) and 1000 m (in right panel), in case of saline zone

Tanta city to the near north of Kafr El Sheikh city (Fig. 14). These two curves can be generalized to the sediments of the Quaternary age along the Nile Valley, especially from the far north of Tanta city to the near north of Kafr El Sheikh city. Also, to the western and eastern parts of the ND, which include brackish groundwater, as well as the areas with the same geologic and hydrogeologic conditions.

Model outputs in case of saline water zone

In this case of VES9 in the saline zone, for illustrating the electrical potential and the density of electric current at the far depths, where the Quaternary aquifer layer (L3) occurs. Also, Fig. 15 shows the electrical potential in the *XZ* view, with focusing on the current density (magenta streamlines) in the *XZ* view, when the spacings between C_1 and C_2 are 300 m (left panel) and 1000 m (right panel). From these Figs, the electric current density is high at shallow depths, when $C_1C_2 = 300$ m, while it is very high in the far depths, when C_1C_2 is 1000 m. Therefore, the electric current in the two cases will be more concentrated at shallow and deep depths, because of the occurrence of high amount of saline groundwater and high content of clay. Accordingly, the electric potential values of the Quaternary aquifer are

very low in this case. Whereas, the electric current density of this zone in this aquifer is very high. In this case, there is a very low resistance for the electric current during its flow through the subsurface materials and this may attenuate and reduce this current during penetration.

Calculation of the electrical potential and apparent resistivity of the saline water zone

Three VESes (VES7, VES8 and VES9) were carried out, assuming the resistivities of the aquifer are 2, 0.5 and 0.1 Ω m, for computing the electrical potential values between the current electrodes (Fig. 16) and calculating the apparent resistivity (Table 8). From the resistivity calculation, there is a sharp decrease in the electrical potential of the aquifer, with decreasing the apparent resistivity values. This is due to the high increase in salinity, for the seawater intrusion and clay content, which increase to the north, and occurred in thin and thick layers in the parts of this zone, as mentioned in the previous hydrogeologic conditions of the aquifer.
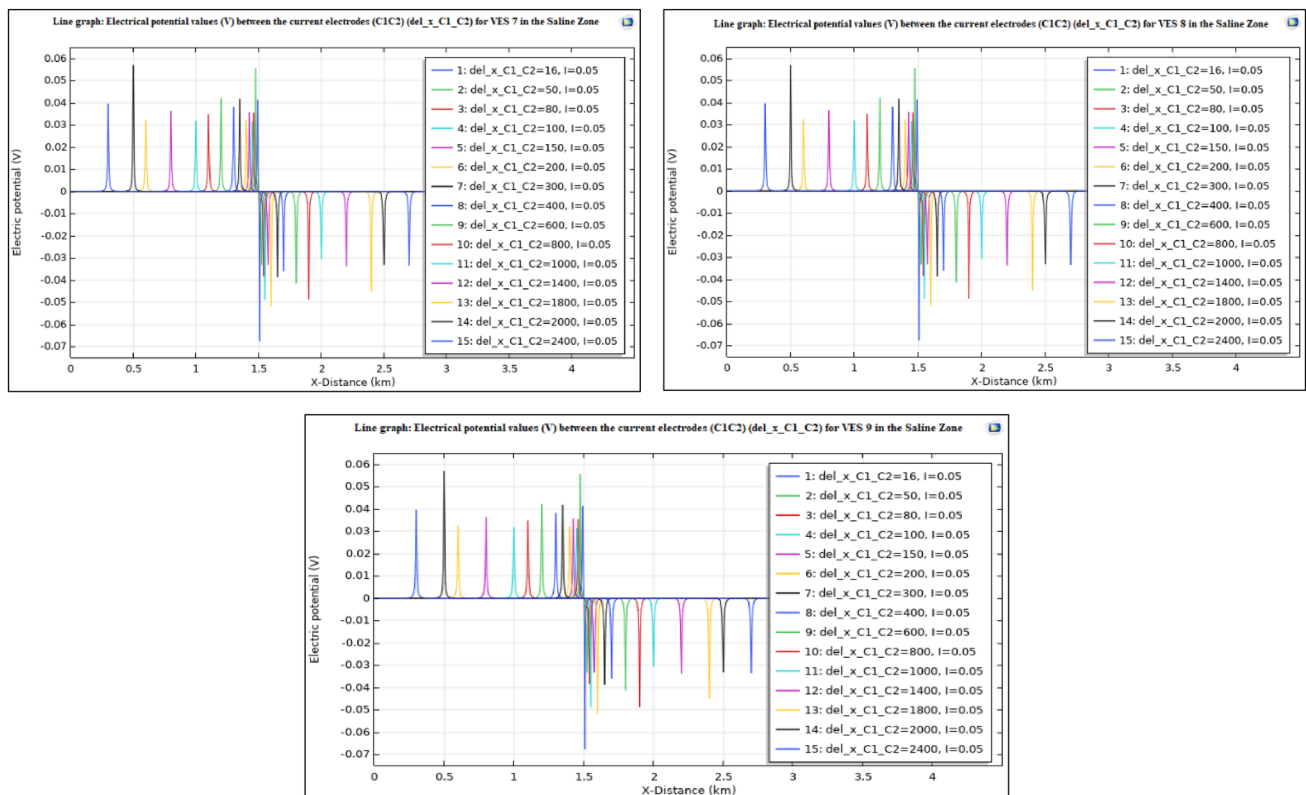
Fig. 16 The electrical potential values between the electrodes of VES7 (upper left panel), VES8 (upper right panel), and VES9 (lower panel), when the resistivities of the aquifer are 2, 0.5 and 0.1 Ω m, respectively, in case of saline zone

Table 8 The electrical potential values and the apparent resistivity values of the brackish zone (VESes 7, 8 and 9), with the subsurface lithologic description

$C_1C_2\backslash 2$ in m	Electrical Potential values (V) of VES7 when aquifer resistivity is 2 Ω m (high Clay with Saline water)	App. resistivity values (Ω m) of VES7 when aquifer resistivity is 2 Ω m (high Clay with Saline water)	Electrical potential values (V) of VES8 when aquifer resistivity is 0.5 Ω m (V. high Clay with high Saline water)	App. resistivity values (Ω m) of VES8 when aquifer resistivity is 0.5 Ω m (V. high Clay with high Saline water)	Electrical potential values (V) of VES9 when aquifer resistivity is 0.1 Ω m (V. high Clay with V. high Saline water)	App. Resistivity values (Ω m) of VES9 when aquifer resistivity is 0.1 Ω m (V. high Clay with V. high Saline water)	Lithology
8	0.009699295	11.5	0.009699295	11.5	0.009699295	11.5	Surface layer
25	0.001272223	8	0.001272223	8	0.001272223	8	
40	0.000164443	4.8	0.000164443	4.8	0.000164443	4.8	
50	7.4918E−05	3.2	7.4918E−05	3.2	7.4918E−05	3.2	
75	1.06757E−05	1.2	1.06757E−05	1.2	1.06757E−05	1.2	Clay
100	4.22111E−06	0.71	4.15501E−06	0.7	4.09156E−06	0.71	
150	1.30794E−06	0.58	1.25799E−06	0.52	1.15231E−06	0.508	
200	1.0137E−06	0.61	8.90492E−07	0.533	7.76737E−07	0.46	Quaternary aquifer
300	4.86249E−07	0.95	3.64772E−07	0.73	2.58472E−07	0.5	
400	5.61356E−07	1.63	5.17809E−07	1.6	3.08507E−07	0.92	
500	6.56142E−07	2.75	5.89512E−07	2.4	3.47313E−07	1.39	
700	9.22013E−07	4.65	8.60602E−07	4.38	4.89363E−07	2.497	
900	1.35469E−06	6.4	1.16881E−06	5.62	6.7602E−07	3.281	
1000	1.4234E−06	6.6	1.24064E−06	5.7	7.3185E−07	3.354	
1200	1.71138E−06	4.8	1.5079E−06	4.3	8.92136E−07	2.55	
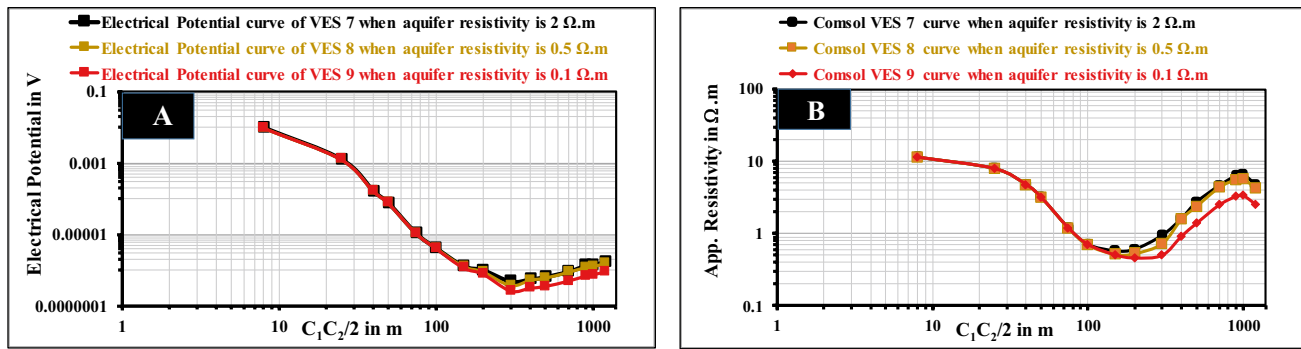
Fig. 17 The electrical potential curves (**A**) ad the apparent resistivity curves (**B**) of VESes 7, 8 and 9, when the aquifer resistivities are 2, 0.5 and 0.1 Ω m, in case of brackish zone

In case of aquifer resistivity is 2 Ω m (VES7)

After computing the electrical potential values of VES7, with the difference at $C_1C_2/2$ (Fig. 16, upper left panel), its electrical potential curve was resulted, as in Fig. 17A, and the apparent resistivity curve was also produced, as in Fig. 17B. The apparent resistivity curve shows that, the apparent resistivity values change with depth, depending on the electrical characteristics of the layers (Table 8) (Fig. 17B). The electrical potential values of the Quaternary aquifer in this case range from 4.86249E–07 V to 1.71138E–06 V. It was noted that, the values of the apparent resistivity decrease sharply, because of the effect of the upper clay layer of the high conductivity, as well as effect of high salinity due to the intrusion of sea water, with considering that, these layer in this zone are saturated with high saline water (Table 8 and Fig. 17B).

Therefore, the higher calculated value of the apparent resistivity of the aquifer was 0.61 Ω m, as a result of the effect of the upper clay layer of the high conductivity (L2), due to the absorption of electric current and to the high effect of salinity and clay content. This effect is higher than in the case of brackish water. While the lower value of the apparent resistivity of this aquifer was 4.8 Ω m, because of the high effect of the sea water invasion and high clay content. These values refer to that, the sediments of this zone are saturated with high saline water and this will effect on the accuracy in defining the lithologic description and the hydro-geoelectrical parameters of the aquifer.

In case of aquifer resistivity is 0.5 Ω m (VES8)

From computing the electrical potential between the electrodes in VES8, as shown in Fig. 16, upper right panel, the values of the electrical potential were determined at each $C_1C_2/2$ (Table 8 and Fig. 17A). It is also resulted in calculating the apparent resistivity values at each $C_1C_2/2$ and

then the VES8 curve represents the saline zone (Table 8 and Fig. 17B). Accordingly, the electrical potential values of the aquifer range from (3.64772E−07 V to 1.5079E−06 V), when the spacings $C_1C_2/2$ are 300 m and 1200 m, respectively. While, the calculated minimum and maximum apparent resistivity values are 0.533 Ω m and 5.7 Ω m, respectively. It was noted that, these values, in case of VES8, are slightly lower than the values in VES7.

In case of aquifer resistivity is 0.1 Ω m (VES9)

Similary, after computing the electrical potential of VES9 (Fig. 16, lower panel), (Table 8 and Fig. 17A), the ρ_a values of this VES were calculated at each $C_1C_2/2$, resulting in an apparent resistivity curve (Fig. 17B). The electrical potential values of the aquifer are ranged from (2.58472E−07 V) to (8.92136E−07 V). While the minimum and maximum apparent resistivity values are varied from 0.46 to 3.353 Ω m, when $C_1C_2/2$ is 200 m and 1000 m, respectively. The previous values indicate also a slight decrease in these values of VES9, as compared to the case of VES8.

Comparison between the electrical potential and apparent resistivity of the saline zone

From the comparison between the computed electrical potential values and the calculated apparent resistivity values of the VESes (VES7, VES8 and VES9) for the saline zone of the Quaternary aquifer (Table 6 and Fig. 17), there is a medium decrease in the values of VES7 and VES8 and high decrease in the values of VES7, VES8 and VES9. This decreasing indicates that, the electrical potential of the aquifer in this zone is high, as affected by the high salinity and high clay content. Therefore, the saline water with high clay content has high influence on the hydro-geoelectrical parameters of the aquifer. Accordingly, the electrical potential and apparent resistivity values are very low in this case. These

Table 9 The average electrical potential values and the apparent resistivity values of the VESes at the saline zone, with the subsurface lithologic description

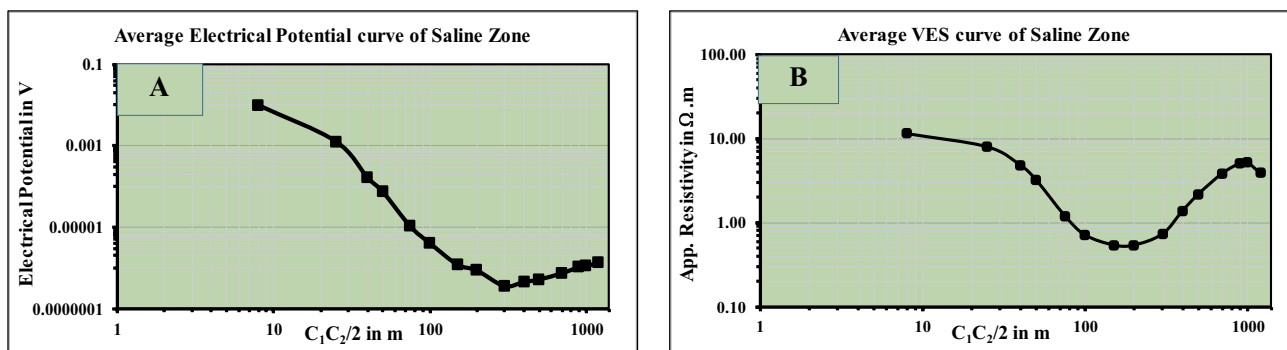| $C_1C_2\backslash2$ in m	Average electrical potential values (V) in saline zone	Average App. resistivity values (Ω m) in saline zone	Lithology
8	0.009699295	11.50	Surface layer
25	0.001272223	8.00	
40	0.000164443	4.80	
50	7.4918E−05	3.20	
75	1.06757E−05	1.20	Clay
100	4.1559E−06	0.71	
150	1.23941E−06	0.54	
200	8.93642E−07	0.53	Quaternary aquifer
300	3.69831E−07	0.73	
400	4.62557E−07	1.38	
500	5.30989E−07	2.18	
700	7.57326E−07	3.84	
900	1.06651E−06	5.10	
1000	1.13197E−06	5.22	
1200	1.37047E−06	3.88	

values are reduced clearly in the case of increase in clay content and saline zone (of VES9). This confirms that, estimating or evaluating the hydro-geoelectric parameters are complex and require a considerable correction. Accordingly, the maximum ranges of the apparent resistivity values are 6.6, 5.7 and 3.353 Ω m, as recorded at the middle depths of the studied aquifer.

Average values of the electrical potential and apparent resistivity of the saline zone sediments

Based on the previous computations, the values of electrical potential and the apparent resistivity in the three previous cases of the saline zone VESes and the average of these values of the Quaternary aquifer in this zone (Table 9), the expected minimum and maximum values of the electrical potential are (3.69831E−07 V) and (1.37047E−06 V),

respectively. While the calculated minimum and maximum values of the apparent resistivity were 0.53 Ω m, due to the influence of the upper clay and high saline water, and 5.22 Ω m, respectively, and to the presence of high clay content, with saline water in the aquifer.

These results also led to the determination of the average electrical potential curve and the average ρ_a curve of the Quaternary layers in the saline zone where the seawater intrusion along the MND, especially from the near north of Kafr El Sheikh city—the near south of Burullus Lake (Fig. 18). These two curves can be generalized to the sediments of the Quaternary age, which are affected by seawater intrusion, especially to the far north of the ND and the near areas of the Mediterranean Sea along the ND. In general, from the far north of Tanta city and exactly to the near south of Kafr El Sheikh city; also, at the northern, western and eastern parts of the ND, which are parallel to this zone and include saline water. Also, all the areas affected by the sea

Fig. 18 The average electrical potential curve (**A**) and the average apparent resistivity curve (**B**) of the VESes, in case of saline zone

water invasion, with the focusing on the shore line, that have the same geologic and hydrogeologic conditions.

Results and discussion

Average values of the electrical potential and apparent resistivity of the three water zones

The computation of the electrical potential values and the calculation of the apparent resistivity values of the shallow layers (L1, L2 and L3) of the Quaternary deposits along the MND in each $C_1C_2/2$ for the VESes in the three zones were an interesting output of this model, as mentioned in the model outputs section. Accordingly, the average electrical potential values of the surface layer (L1) the clay layer (L2), and the Quaternary aquifer layer (L3), as well as the calculated average apparent resistivity values of these layers were determined, as shown in Table 10. The max and min values of the electrical potential of the first layer are (0.146901943 V) and (0.001042753 V) in the fresh zone, (0.096961783 V) and (0.000697632 V) in the brackish zone, and (0.009699295 V) and (7.4918E−05 V) in the saline zone, respectively. The max and min values of the electrical potential of the layer of clay are (0.000122068 V) and (1.0903E−05 V) in the fresh zone, (8.45968E−05 V) and (7.97051E−06 V) in the brackish

zone, and (1.06757E−05 V) and (1.23941E−06 V) in the saline zone, respectively. While the min and max values of the electrical potential of the aquifer are (4.36914E−06 V) and (1.74532E−05 V) in the fresh zone, (3.0436E−06 V) and (1.02057E−05 V) in the brackish zone, and (3.69831E−07 V) and (1.37047E−06 V) in the saline zone, respectively (Table 10).

According to the previous average values of the electrical potential of the aquifer, the general average values are (1.0904E−05 V), in the fresh zone, (6.15462E−06 V), in the brackish zone and (8.22911E−07 V) in the saline zone. Similarly, the average values of the apparent resistivity of the Quaternary aquifer layer are (5.5 and 59) Ω m in the fresh zone, (3.57 and 39.17) Ω m in the brackish zone, and (0.53 and 5.22) Ω m in the saline zone, respectively. From the average values of the electrical potential and apparent resistivity to the VESes of the three zones, as shown in Table 10, the average curve of these VESes in each zone were represented, as a curve for each zone, as shown in Fig. 19.

Also, there is a slight decrease in the values of the fresh zone to the brackish zone, because of the slight effect of the brackish water and medium content of clay, and a significant reduce in the values from the fresh/brackish zone to the saline zone, due to influence of high salinity and high clay content. The decreasing of these values appears clearly in the northern locations along the MND.

Table 10 The average electrical potential values and the apparent resistivity values of the fresh, brackish, and saline zones VESes, with the subsurface lithologic description

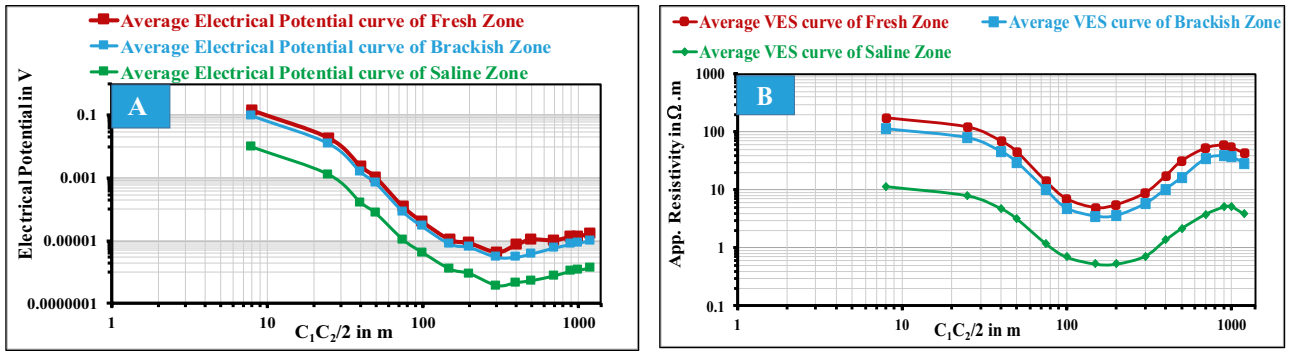| $C_1C_2/2$ in m	Average electrical potential values (V) in fresh zone	Average App. Resistivity values (Ω m) in fresh zone	Average electrical potential values (V) in brackish zone	Average App. resistivity values (Ω m) in brackish zone	Average electrical potential values (V) in saline zone	Average App. resistivity values (Ω m) in saline zone	Lithology
8	0.146901943	174	0.096961783	114	0.009699295	11.5	Surface layer
25	0.019064522	121	0.012604861	80	0.001272223	8	
40	0.002377464	69	0.001581079	46	0.000164443	4.8	
50	0.001042753	45	0.000697632	30	7.4918E−05	3.2	
75	0.000122068	14	8.45968E−05	10	1.06757E−05	1.2	Clay
100	3.99539E−05	7	2.87042E−05	4.8	4.1559E−06	0.71	
150	1.0903E−05	4.9	7.97051E−06	3.5	1.23941E−06	0.54	
200	8.56301E−06	5.5	6.29089E−06	3.57	8.93642E−07	0.53	Quaternary aquifer
300	4.36914E−06	8.77	3.0436E−06	5.73	3.69831E−07	0.73	
400	7.53245E−06	17.27	3.10857E−06	10.27	4.62557E−07	1.38	
500	1.11367E−05	31.33	3.90479E−06	16.30	5.30989E−07	2.18	
700	1.05655E−05	52.33	6.07505E−06	34.67	7.57326E−07	3.84	
900	1.36289E−05	59	7.88527E−06	39.17	1.06651E−06	5.10	
1000	1.39827E−05	54	8.72312E−06	37.67	1.13197E−06	5.22	
1200	1.74532E−05	42.5	1.02057E−05	28.83	1.37047E−06	3.88	
General Av. EP of Aquifer	1.0904E−05		6.15462E−06		8.22911E−07		

Fig. 19 The average electrical potential curves (**A**) and the average apparent resistivity curves (**B**) of the fresh, brackish and saline zones VESes

Determination of the coefficient of decreasing in the electrical potential (V_{cd}) and apparent resistivity (ρ_{cd})

Determination of the coefficient of decreasing in the electrical potential (V_{cd}) and the apparent resistivity (ρ_{cd}) will be calculated by using the following formulas:

$$V_{cd} = \frac{V_{FZ}}{V_{BZ}}. \tag{8}$$

Formula (8) is used for determining the coefficient of decreasing in the electrical potential of the Quaternary aquifer from the fresh zone to the brackish zone.

Where V_{FZ} is the electrical potential of the fresh zone (V) and V_{BZ} is the electrical potential of the brackish zone (V).

$$V_{cd} = \frac{V_{BZ}}{V_{SZ}}. \tag{9}$$

Formula (9) is used for determining the coefficient of decreasing in the electrical potential of the Quaternary aquifer from the brackish zone to the saline zone.

Where V_{SZ} is the electrical potential of the saline zone (V).

$$V_{cd} = \frac{V_{FZ}}{V_{SZ}}. \tag{10}$$

Formula (10) is used for determining the coefficient of decreasing in the electrical potential of the Quaternary aquifer from the fresh zone to the saline zone.

$$\rho_{a(cd)} = \frac{\rho_{a(FZ)}}{\rho_{a(BZ)}}. \tag{11}$$

Formula (11) is used for determining the coefficient of decreasing in the apparent resistivity ($\rho_{a(cd)}$) of the Quaternary aquifer from the fresh zone to the brackish zone.

Where $\rho_{a(FZ)}$ is the ρ_a of the fresh zone (Ω m) and $\rho_{a(BZ)}$ is the ρ_a of the brackish zone (Ω m).

$$\rho_{a(cd)} = \frac{\rho_{a(BZ)}}{\rho_{a(SZ)}}. \tag{12}$$

Formula (12) is used for determining the coefficient of decreasing in apparent resistivity ($\rho_{a(cd)}$) of this aquifer from brackish to saline zone.

Where $\rho_{a(FZ)}$ is the apparent resistivity of the saline zone (Ω m).

$$\rho_{a(cd)} = \frac{\rho_{a(FZ)}}{\rho_{a(SZ)}}. \tag{13}$$

Formula (13) is used for determining the coefficient of decreasing in the apparent resistivity ($\rho_{a(cd)}$) of the Quaternary aquifer from the fresh zone to the saline zone.

The previous formulas were applied for determining the coefficients of decreasing in both the electrical potential and ρ_a values of the three water zones, depending on the average values of the electrical potential and ρ_a of the VESes of the three water zones, as shown reported in the previous Tables 5, 7 and 9. Accordingly, the values of the coefficient of decreasing of L1, L2 and L3 at each $C_1C_2/2$, were calculated, as in Table 11. In this study, the focusing will be on the average values of the coefficient of decreasing of the Quaternary aquifer. Whereas the average values of the coefficient of decreasing in the electrical potential are 1.86, 7.49 and 13.81, in the case of change from the fresh zone to the brackish zone, from the brackish zone to the saline zone, and from the fresh zone to saline zone, respectively.

Table 11 Coefficients of decreasing in the electrical potential and the apparent resistivity values of the fresh, brackish and saline zones VESes with the subsurface lithologic description

$C_1C_2\backslash2$ in m	Coefficient of decreasing in E. Potential (V_{cd}) in case of F.Z. and B.Z	Coefficient of decreasing in app. resistivity (ρ_{cd}) in case of F.Z. and B.Z	Coefficient of decreasing in E. Potential (V_{cd}) in case of B.Z. and S.Z	Coefficient of decreasing in app. resistivity (ρ_{cd}) in case of B.Z. and S.Z	Coefficient of decreasing in E. Potential (V_{cd}) in case of F.Z. and S.Z	Coefficient of decreasing in app. resistivity (ρ_{cd}) in case of F.Z. and S.Z	Lithology
8	1.52	1.53	10	9.91	15.15	15.13	S. layer
25	1.51	1.51	9.91	10	14.99	15.13	
40	1.50	1.50	9.61	9.58	14.46	14.38	
50	1.49	1.50	9.31	9.38	13.92	14.06	
75	1.44	1.40	7.92	8.33	11.43	11.67	Clay
100	1.39	1.46	6.91	6.79	9.61	9.91	
150	1.37	1.40	6.43	6.53	8.80	9.14	
200	1.36	1.54	7.04	6.67	9.58	10.29	Quaternary aquifer
300	1.44	1.53	8.23	7.89	11.81	12.06	
400	2.42	1.68	6.72	7.42	16.28	12.48	
500	2.85	1.92	7.35	7.48	20.97	14.37	
700	1.74	1.51	8.02	9.02	13.95	13.62	
900	1.73	1.51	7.39	7.68	12.78	11.57	
1000	1.60	1.43	7.71	7.22	12.35	10.35	
1200	1.71	1.47	7.45	7.42	12.74	10.94	
Average of coefficient of decreasing of Aquifer	1.86	1.57	7.49	7.6	13.81	11.96	

Effect of variation of salinity and clay content on the electrical potential of the aquifer

Similarly, in the case of apparent resistivity, the values of the coefficient of decreasing are 1.57, 7.6 and 11.96, respectively. Accordingly, the high average values were calculated in the case of decreasing in the electrical potential and the apparent resistivity from the fresh zone to the saline zone. The medium average value was calculated in the case of decreasing in the electrical potential and apparent resistivity from brackish to saline zone. Also, these calculations appeared that, there is a low coefficient value from the fresh zone to the brackish zone, because of the little effect of the salinity and low content of clay on the electrical potential values in the two zones. There is a high coefficient value from the fresh zone to the saline zone because the high effect of the high clay content and high salinity, and this coefficient rises northward toward the Mediterranean Sea.

For determining and understanding the salinity and clay content variation effect on the electrical potentials of the Quaternary aquifer in the three zones, it should be calculated the rate of decreasing in the electrical potential values, through comparing the values of electrical potential in the three zones with the values of electrical potential in the fresh zone, with clean sediments. Therefore, it can be calculated the rate of decreasing (R_d) from the following formulas (14 or 15):

$$R_d = 1 - \frac{V2}{V1}, \tag{14}$$

where $V1$ is the electrical potential of VES1 in the fresh zone and $V2$ is the electrical potential values of the different VESes from VES3 to VES9 in the three zones.

Or from the following formula (15)

$$R_d = \frac{Q_d}{V1}, \tag{15}$$

where Q_d is the amount of decreasing (V), ($Q_d = V1 - V2$).

Table 12 A comparison between the electrical potential values of the aquifer, when the assumed aquifer resistivities are 90 Ω m (fresh zone) and 20 Ω m (fresh zone with low clay content) and calculating the coefficient of decreasing, the amount of decreasing and the rate of decreasing

$C_1C_2\backslash2$ in m	Electrical Potential (V_1) values (V) of VES1 when aquifer resistivity is 90 Ω m (Fresh zone with Pure Sediments)	Electrical Potential (V_2) values (V) of VES3 when aquifer resistivity is 20 Ω m (Fresh zone with Low Clay)	Coefficient of decreasing in E. Potential (V_{cd}) ($V1/V2$)	Amount of decreasing (reducing), (Q_d) ($V1 - V2$) in (V)	Rate of decreasing (reducing) (R_d) in V (V)	Rate of decreasing (reducing) (R_d) in V (%)
200	8.85444E−06	8.248E−06	1.07	0.0000006	0.0684855	6.85
300	4.68614E−06	4.0309E−06	1.16	0.0000007	0.1398309	13.98
400	9.0491E−06	6.557E−06	1.38	0.0000025	0.2753952	27.54
500	1.34485E−05	9.2505E−06	1.45	0.0000042	0.3121512	31.22
700	1.3899E−05	9.2017E−06	1.51	0.0000047	0.3379604	33.80
900	1.69609E−05	1.1519E−05	1.47	0.0000054	0.3208523	32.09
1000	1.82343E−05	1.2583E−05	1.45	0.0000057	0.3099243	30.99
1200	2.02917E−05	1.4703E−05	1.38	0.0000056	0.2754345	27.54
Average	1.3178E−05	9.51161E−06	1.36	0.0000037	0.2550043	25.50%

Also, it can be calculated the rate of decreasing (R_d) in percentage (%), using the previous formulas (14 or 15) by multiplying by 100.

Calculation of the rate of decreasing in the electrical potential

From the fresh zone with clean sediments to the fresh zone with low clay content

From the comparison of the electrical potential of the aquifer in the case of VES1, in the fresh zone with clean sediments ($V1$), and in the case of VES3, in the fresh zone with low clay content ($V2$), using the previous formulas, the following was calculated: the coefficient of decreasing in the electrical potential of the aquifer ($\frac{V2}{V1}$), the amount of decreasing (Q_d) (V), and the rate of decreasing (R_d) (V, %), as shown in Table 12. It was found that, the min and max values of the coefficient of decreasing are (1.07) and (1.51), respectively. The values of the decreasing rate range from (0.0684855 V) (6.85%) to (0.3379604 V) (33.8%). The average values of the coefficient of decreasing and rate of decreasing are (1.36) and (0.2550043 V) (25.50%), respectively. These values indicate that, the effect of low content of clay in reducing the electrical potential in the same zone is weak. This reflects that, the low clay content, as only one influence factor in the electrical potential, affected the reduction of the electrical potential values of the Quaternary aquifer by 25.50%. This,

Table 13 A comparison between the electrical potential values of the aquifer, when the assumed aquifer resistivities are 90 Ω m (fresh zone) and 10 Ω m (brackish zone with medium clay content) and calculating the coefficient of decreasing, the amount of decreasing and the rate of decreasing

$C_1C_2\backslash2$ in m	Electrical Potential ($V1$) values (V) of VES1 when aquifer resistivity is 90 Ω m (Fresh zone with Pure Sediments)	Electrical Potential ($V2$) values (V) of VES5 when aquifer resistivity is 10 Ω m (medium Clay with Brackish water)	Coefficient of decreasing in E. Potential (V_{cd}) ($V1/V2$)	Amount of decreasing (reducing), (Q_d) ($V1-V2$) in (V)	Rate of decreasing (reducing) (R_d) in V (V)	Rate of decreasing (reducing) (R_d) in V (%)
200	8.85444E−06	6.00684E−06	1.47	0.0000028	0.321601543	32.16
300	4.68614E−06	2.83359E−06	1.65	0.0000019	0.395326232	39.53
400	9.0491E−06	4.44635E−06	2.04	0.0000046	0.508641762	50.86
500	1.34485E−05	3.92899E−06	3.42	0.0000095	0.707849502	70.78
700	1.3899E−05	6.12863E−06	2.27	0.0000078	0.559060971	55.91
900	1.69609E−05	8.26404E−06	2.05	0.0000087	0.512759603	51.28
1000	1.82343E−05	8.84073E−06	2.06	0.0000094	0.515159873	51.52
1200	2.02917E−05	1.01017E−05	2.01	0.0000102	0.502177184	50.22
Average	1.3178E−05	6.31885E−06	2.12	0.0000069	0.502822084	50.28%

also, reflects a slight difference between the electrical potential and the ρ_a values in the cases of VES1 and VES3 and during the hydro-geoelectric parameters evaluation.

From the fresh zone with clean sediments to the brackish zone with medium clay content

From the comparison of the electrical potential of the aquifer in the case of VES1, in the fresh zone (V1), and VES5 in the brackish zone with medium clay content (V2), for calculating the coefficient of decreasing in the electrical potential of the aquifer, the amount of decreasing and the rate of decreasing (Table 13). It was found that, the min and max values of the coefficient of decreasing are (1.47) and (3.42), respectively. The min and max values of the rate of decreasing are (0.321601543 V) (32.16%) and (0.707849502 V) (70.78%), respectively. The average values of the coefficient of decreasing and the rate of decreasing are (2.12) and (0.502822084 V) (50.28%), respectively. These values indicate that, the effect of medium salinity and clay content in the reduction of the electrical potential in the brackish zone is medium. This reflects that, both factors influence in reducing the electrical potential values of the Quaternary aquifer by 50.28%. Also, there is a medium difference between the values of the electrical potential and the apparent resistivity in the cases of VES1 and VES5 and during the evaluation of the hydro-geoelectrical parameters too.

From the fresh zone with clean sediments to the brackish zone with medium to high clay content

Similarly, the coefficient of decreasing in the electrical potential of the aquifer, the amount of decreasing and the rate of decreasing (Table 14), were calculated from the comparison of the electrical potential of the aquifer in the case of VES1, of the fresh zone with pure sediments (clean zone) (V1) and in the case of VES6 of the brackish zone with high clay content (V2). Therefore, the min and max values of the coefficient of decreasing are (1.33 and 3.59), respectively, of the decreasing rate are (0.246159678 V) (24.62%) and (0.721365322 V) (72.14%), respectively. The average values of the coefficient of decreasing and the rate of decreasing are (2.38) and (0.529091299 V) (52.91%), respectively. Although there is brackish water and high content of clay in the aquifer, however, the reduction of the electrical potential of the Quaternary aquifer in the brackish zone is slightly (52.91%), as compared with the previous case (of VES1 and VES5). Accordingly, there is a little difference between the values of the electrical potential and apparent resistivity in the cases of VES5 and VES6.

From the fresh zone with clean sediments to the saline zone with high clay content

From the comparison of the electrical potential of the aquifer in the case of VES1, of the fresh zone with pure sediments (V1) in the case of VES7 of the saline zone with high clay content (V2), as shown in Table 15, it was found that, the min and max values of the coefficient of decreasing are (8.73) and (20.49), respectively, and the min and max values of the rate of decreasing are (0.885515302 V) (88.55%) and (0.95121079 V) (95.12%), respectively. The average values of the coefficient of decreasing and the rate of decreasing are (13.41) and (0.92029003 V) (92.03%), respectively. These values give an indication about the high effect resulted from the saline water and high clay content in reducing the electrical potential of the saline zone. This reflects that, both

Table 14 A comparison between the electrical potential values of the aquifer, when the assumed aquifer resistivities are 90 Ω m (fresh zone) and 5 Ω m (brackish zone with high clay content) and calculating the coefficient of decreasing, the amount of decreasing and the rate of decreasing

$C_1C_2/2$ in m	Electrical Potential ($V1$) values (V) of VES1 when aquifer resistivity is 90 Ω m (Fresh zone with Pure Sediments)	Electrical Potential ($V2$) values (V) of VES6 when aquifer resistivity is 5 Ω m (high Clay with Brackish water)	Coefficient of decreasing in E. Potential (V_{cd}) ($V1/V2$)	Amount of decreasing (reducing), (Q_d) ($V1 - V2$) in (V)	Rate of decreasing (reducing) (R_d) in V (V)	Rate of decreasing (reducing) (R_d) in V (%)
200	8.85444E−06	6.67483E−06	1.33	0.0000022	0.246159678	24.62
300	4.68614E−06	3.27104E−06	1.43	0.0000014	0.301975307	30.20
400	9.0491E−06	2.52139E−06	3.59	0.0000065	0.721365322	72.14
500	1.34485E−05	3.75041E−06	3.59	0.0000097	0.72112815	72.11
700	1.3899E−05	5.59243E−06	2.49	0.0000083	0.597639056	59.76
900	1.69609E−05	7.18461E−06	2.36	0.0000098	0.576401862	57.64
1000	1.82343E−05	8.45951E−06	2.16	0.0000098	0.536066625	53.61
1200	2.02917E−05	9.49664E−06	2.14	0.0000108	0.531994396	53.20
Average	1.3178E−05	5.86886E−06	2.38	0.0000073	0.529091299	52.91%

Table 15 A comparison between the electrical potential values of the aquifer when the assumed aquifer resistivities are 90 Ω m (fresh zone) and 2 Ω m (saline zone with high clay content) and calculating the coefficient of decreasing, the amount of decreasing, and the rate of decreasing

$C_1C_2\backslash2$ in m	Electrical Potential ($V1$) values (V) of VES1 when aquifer resistivity is 90 Ω m (fresh zone with pure sediments)	Electrical potential ($V2$) values (V) of VES7 when aquifer resistivity is 2 Ω m (high Clay with saline water)	Coefficient of decreasing in E. Potential (V_{cd}) ($V1/V2$)	Amount of decreasing (reducing), (Q_d) ($V1 - V2$) in (V)	Rate of decreasing (reducing) (R_d) in V (V)	Rate of decreasing (reducing) (R_d) in V (%)
200	8.85444E−06	1.0137E−06	8.73	0.0000078	0.885515302	88.55
300	4.68614E−06	4.8625E−07	9.64	0.0000042	0.896236767	89.62
400	9.0491E−06	5.6136E−07	16.12	0.0000085	0.937965518	93.80
500	1.34485E−05	6.5614E−07	20.49	0.0000128	0.95121079	95.12
700	1.3899E−05	9.2201E−07	15.07	0.0000130	0.93366353	93.37
900	1.69609E−05	1.3547E−06	12.52	0.0000156	0.920128887	92.01
1000	1.82343E-05	1.4234E−06	12.81	0.0000168	0.92193819	92.19
1200	2.02917E−05	1.7114E−06	11.86	0.0000186	0.915661253	91.57
Average	1.3178E−05	1.01612E−06	13.41	0.0000122	0.92029003	92.03%

Table 16 A comparison between the electrical potential values of the aquifer when the assumed aquifer resistivities are 90 Ω m (fresh zone) and 0.1 Ω m (saline zone with very high clay content) and calculating the coefficient of decreasing, the amount of decreasing, and the rate of decreasing

$C_1C_2/2$ in m	Electrical Potential ($V1$) values (V) of VES1 when aquifer resistivity is 90 Ω m (fresh zone with pure sediments)	Electrical Potential ($V2$) values (V) of VES9 when aquifer resistivity is 0.1 Ω m (high Clay with saline water)	Coefficient of decreasing in E. Potential (V_{cd}) ($V1/V2$)	Amount of decreasing (reducing), (Q_d) ($V1 - V2$) in (V)	Rate of decreasing (reducing) (R_d) in V (V)	Rate of decreasing (reducing) (R_d) in V (%)
200	8.85444E−06	7.76737E−07	11.39	0.0000081	0.912277117	91.23
300	4.68614E−06	2.58472E−07	18.13	0.0000044	0.944843309	94.48
400	9.0491E−06	3.08507E−07	29.33	0.0000087	0.965907379	96.59
500	1.34485E−05	3.47313E−07	38.72	0.0000131	0.974174568	97.42
700	1.3899E−05	4.89363E−07	28.40	0.0000134	0.964791579	96.48
900	1.69609E−05	6.7602E−07	25.09	0.0000163	0.960142438	96.01
1000	1.82343E−05	7.3185E−07	24.92	0.0000175	0.959864131	95.99
1200	2.02917E−05	8.92136E−07	22.75	0.0000194	0.9560345	95.60
Average	1.3178E−05	5.6005E−07	24.84	0.0000126	0.954754377	95.47%

factors had a significant effect in reducing the electrical potential values of this aquifer by (92.03%) in the saline zone. This significant and obvious effect of the saline water and clay content of this zone in the case of VES1 and VES7 of reducing the electrical potential will lead to a high significant difference during the hydro-geoelectric parameters evaluation.

From the fresh zone with clean sediments to the saline zone with very high clay content

Also, from the comparison of the electrical potential of the aquifer in the case of VES1, of the fresh zone with clean sediments ($V1$), and VES9, of the saline zone with very high clay content ($V2$), as shown in Table 16, it was found that, in the case of the min and max values of the coefficient of decreasing are (11.39) and (38.72), respectively, the min and max values of the rate of decreasing are (0.912277117 V) (91.23%) and (0.974174568 V) (97.42%), respectively. The average values of the coefficient of decreasing and the rate of decreasing are (24.84) and (0.954754377 V) (95.47%), respectively. These values indicate that, the high salinity of the water, as well as the very high content of the clay have a strong effect in reducing the electrical potential of the Quaternary aquifer, with a percentage of 95.47% in the zone under study. Also, such a large effect, in this case, will lead to a very large difference during the evaluation of the hydro-geoelectrical parameters.
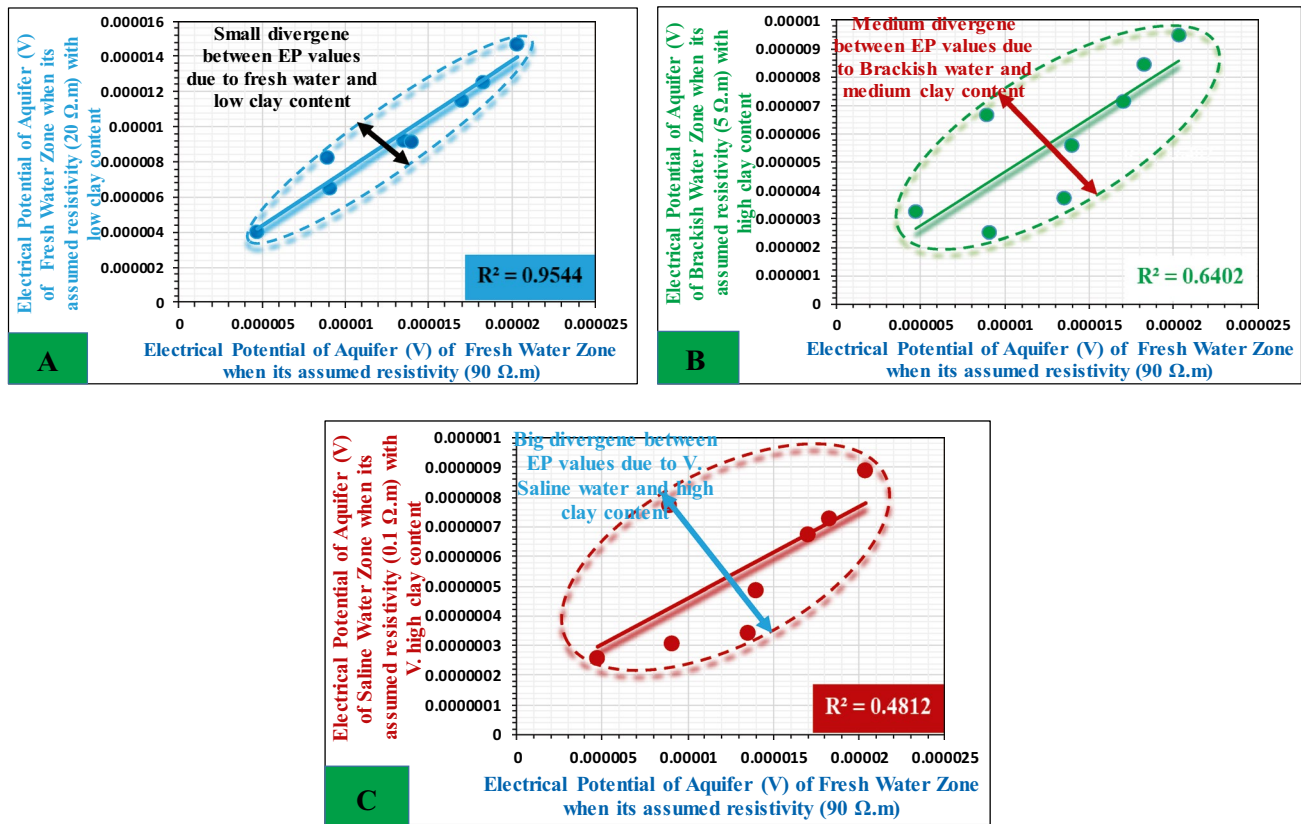
Fig. 20 Effect of salinity and clay content on the correlation coefficient (R^2) between: the electrical potential values of the Quaternary aquifer of the fresh zone (when the assumed resistivities are 90 Ω m and 20 Ω m) (**A**), the electrical potential values of the Quaternary aquifer of the fresh zone (when the assumed resistivity is 90 Ω m) and the brackish zone (when the assumed resistivity is 5 Ω m) (**B**), and the electrical potential values of the Quaternary aquifer of the fresh zone (when the assumed resistivity is 90 Ω m) and the saline zone (when the assumed resistivity is 0.1 Ω m) (**C**)

Effect of salinity and clay content on the correlation coefficient between the different electrical potential values of the Quaternary aquifer

The values of the correlation coefficient (R^2) are an interesting statistical evaluation of the relationship between any two variables, to measure the strength of the relationship between both variables. Accordingly, it was shown formerly how the degree of salinity and clay content affected the relationships between the electrical potential values in the three zones of the Quaternary aquifer, through the correlation coefficient, as shown in Fig. 20. Therefore, the resulting value of the correlation coefficient from the relationship between the electrical potential values in the fresh zone with clean sediments and in the fresh zone with low clay content (Fig. 20A) is $R^2 = 0.9544$ (95.44%). According to the previous value of R^2, the effect of low clay content on the measurements of resistivity and other geophysical and hydrogeologic parameters, estimated from the DC-resistivity method in this zone of the Quaternary aquifer, is about 0.05 (5%) error.

The resulting value of the correlation coefficient from the relationship between the computed values of the electrical potential in the fresh water zone with pure sediments and the computed values of the electrical potential in the brackish zone of the Quaternary aquifer (Fig. 20B) is $R^2 = 0.6402$ (64.02%). This means that, around 0.36 (36%) error in the measurement and determination of the true resistivity measurements and the other geophysical and hydrogeologic parameters, estimated from the DC-resistivity method (VES) in the brackish zone of the Quaternary aquifer is due to the effect of medium to high clay content and medium salinity (brackish water) in the mixed water zone between the fresh zone from Nile river and the salt zone from seawater intrusion (mixed zone or transition zone).

Also, the resulting value of the correlation coefficient, from the relationship between the computed values of the electrical potential in the fresh water zone with pure sediments and the computed values of the electrical potential in the saline water zone of the Quaternary aquifer (Fig. 20C) is $R^2 = 0.4812$ (48.12%). This gives an indication of about 0.52 (52%) error in the determination of the true measurements

Fig. 21 Comparison between the electrical potential curves of the Quaternary aquifer in the three water zones
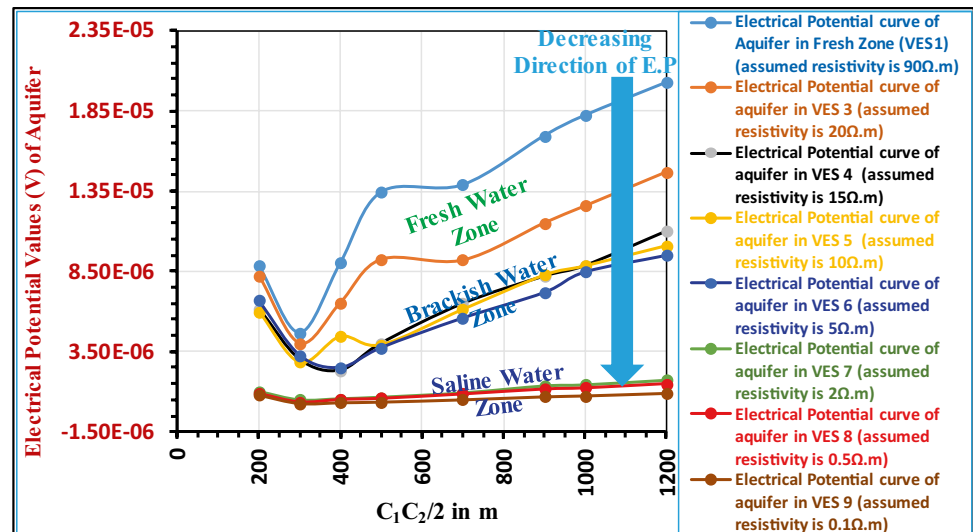
of the resistivity and the other geophysical and hydrogeologic parameters, estimated from the DC-resistivity method (VES) in the saline zone. Such a conclusion can be extended to the soil description of the Quaternary aquifer, because of the high clay content and high salinity effect in the saline water zone, in which this error increases with the increase of salinity and clay content, as we go far north along the MND toward the Mediterranean Sea.

Comparison between the electrical potential values of the quaternary aquifer in the three water zones

Depending on calculating the values of the electrical potential of the aquifer in the three water zones, at each change of the spacing between the electrodes of the electric current, as in the previous Tables, which starts from 200 m, the spacing at which the recording of the groundwater aquifer begins, to 1200 m, the spacing at which the last depths of the this aquifer, which is the top of Pliocene clay layer, has been plotted in the form of electric potential curves for each zone, as shown in Fig. 21. It was noted from the values and curves of the electrical potential that, the values of the electrical potential of the fresh zone are higher than the values of the electric potential of the brackish zone, especially at the beginning, when the spacing between the electrodes of the electric current was 400 m, the spacing at which the recording of depths inside the aquifer begins, that was not affected by the influence of clay layer above it (Fig. 21). Also, it was observed that, the layer of clay above the aquifer affects by the same degree on the electrical potential values of the previous two zones, especially when the spacings between the current electrodes $C_1C_2/2$ are 200 m and 300 m. This indicates that, the real values of the electrical potential, as well as the true electrical resistivity start, when $C_1C_2/2$ is 400 m.

Therefore, the values of the electrical potential and the values of the electrical resistivity of this aquifer should be avoided up to this spacings for determining its electrical and hydrogeologic properties because, it is affected by the layer of clay covering it. Also, through the potential curves of the previous two zones, it was found that, the electrical potential values of the fresh zone are quickly affected by the presence of clay because its TDS value is low, and there is a small difference in the values of the electric potential for the brackish water layer. This last case is analogous to the case of the electrical potential values of the salt zone and the values of the electrical potential in this zone are very few, compared to the previous two zones and these values are different very little among themselves through the increase in the spacing between the current electrodes and represent a straight line (Fig. 21). From the foregoing observation, it can be shown that, the values of electrical resistivity, as well as other electrical and hydrogeologic parameters, that can be calculated from the DC-resistivity method, differ greatly from one zone to another and they are slightly varied within each zone.

## Electrical potential and apparent resistivity cross sections

Depending on the calculated values of the electrical potential and the apparent electrical resistivity of the sediments of the Quaternary age represented in the shallow layers (L1, L2 and L3) down to the fourth Pliocene clay layer (L4), that located at the bottom of the aquifer across the different water ranges, as previously explained in detail in the former sections and reported in the foregoing Tables and Figs., that are represented by the nine VESes from VES1 to VES9, we were able to represent the calculated and expected electrical potential values for the MND area in the form of a two-dimensional cross section (2D), from S to N direction,
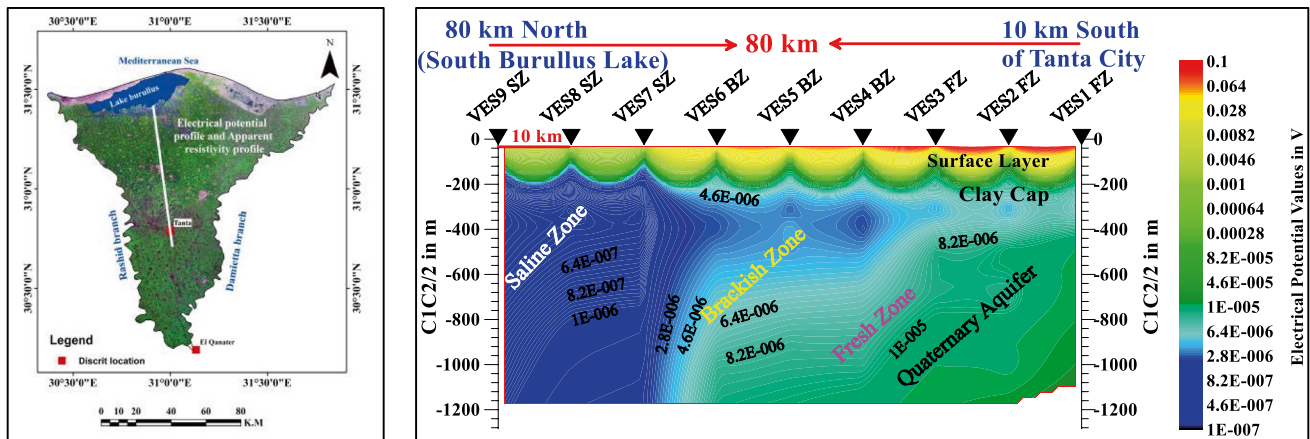
Fig. 22 The MND area map, with the suggested cross section of the electrical potential and apparent resistivity (left panel), passing through the three water zones, along the MND tract. Cross section of the electrical potential with $C_1C_2/2$ (m) from 10 km south of Tanta city to the south of Burullus Lake, with a total length of ~80 km (right panel)

Fig. 23 A cross-section of the apparent resistivity with $C_1C_2/2$ (m) along the MND are from 10 km south of Tanta city to the south of Burullus Lake, with a total length of ~80 km
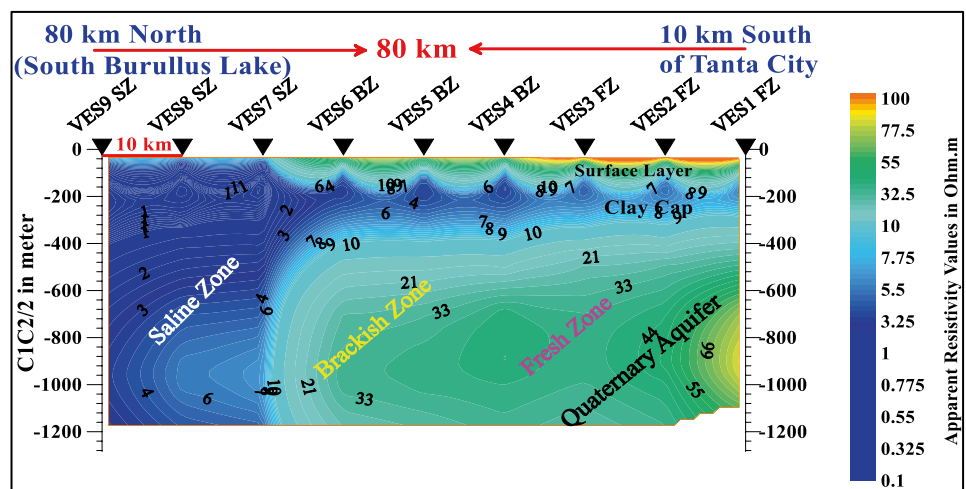
with a length of 80 km (Fig. 22, left panel) and the section of Fig. 22, right panel. Also, we were able to represent the calculated and expected apparent electrical resistivity values for the MND area, in the form of a two-dimensional cross section, from south to north (Fig. 23).

These two previous cross sections painted a very expressive picture of the hydrogeologic situation and the expected shape of the three water zones, from the south (where the fresh zone occurs) to the north (where the salt zone lies, as affected by the interference of the salty saline water into the fresh water) through the gradation of the electrical potential values or the apparent electrical resistivities. Accordingly, the two-dimensional electrical potential cross section (Fig. 22, right panel) has shown that, the values of this electrical potential are decreasing from south to north and also the two-dimensional apparent resistivity cross-section has clarified that, decrease in values and their direction (Fig. 23).

These two cross-sections showed the existence of a clear gradation in these values from south to north, and this gradation clearly beneficial for separating the zones, especially the fresh water zone and the saline water zone along the middle part of the ND; while the seawater-fresh water mixing zone (transition zone) requires high accuracy to define it from these values.

These two cross-sections also showed a sharp drop in the values of the electrical potential and the apparent electrical resistivity, when entering directly into the salt zone. The values of the electrical potential showed that, it is expected that, there is a sharp and severe change in the chemical properties of water from the south to the north, especially (TDS), which led to a severe change in the electrical properties and then in the hydrogeologic properties of the sediments of the Quaternary aquifer. These characteristics are believed from the south toward the north. Also, the expected interval between

the brackish zone and the saline zone is after ~ 40 km from Tanta city and that, the brackish zone starts after 20 km from Tanta city and increases northerly across the MND area.

Conclusion

Salinity and clay content are strong factors in affecting the hydro-geoelectric properties of the porous sediments, such as the electrical resistivity or conductivity. In this study, COMSOL MNM was used for simulating these parameters to monitor the salinity-clay variation effect on the electrical potential of the Quaternary aquifer, by applying the DC-resistivity technique (VESes), through the evaluated shallow section in three different water zones, along the MND tract of Egypt. The model includes four different geologic layers L1, L2, L3 and L4 in their lithologies and assumed resistivities, in which L3 refers to the studied Quaternary aquifer. Nine VESes were performed, for computing the electrical potential and calculating the apparent resistivity of the Quaternary sediments (L1–L3), that focusing on the Quaternary aquifer. The electrical potential and apparent resistivity curves of these layers were established.

The results of the model appeared the minimum, maximum and average values of the electrical potential and apparent resistivity for each layer in the three water zones. The apparent resistivity ρ_a values are ranged between (5.5) and (59) Ω m in the fresh zone, from (3.57) to (39.17) Ω m in the brackish zone, and from (0.53) to (5.22) Ω m in the saline zone. These values referred to a slight decrease from the fresh zone to the brackish zone and a significant decrease from the fresh and brackish zones to the saline zone. The coefficient and rate of decreasing in the electrical potential of this aquifer were calculated, as well as their average values were calculated. The resulted values of the correlation coefficients inferred from the relationship between the electrical potential values in the fresh, brackish and saline zones, reflected ~ 0.05 (5%), ~ 0.36 (36%) and ~ 0.52 (52%), as the expected errors in the field measurements of resistivity, in estimating the hydro-geoelectric parameters, and describing the lithologies from the DC-resistivity method in the fresh, brackish and saline zones, respectively, that increases with increasing the salinity and clay content.

Finally, the hydrogeophysic parameters, that can be calculated from the DC-resistivity method, differ greatly from a zone to another, but it is varied slightly within each zone. 2D cross-sections of the electrical potential and apparent resistivity values showed the existence of a clear gradation in these values and have clearly benefited in identifying and separating the fresh zone from the saline zone, while the transition zone between them requires high accuracy in separating it. This simulation is considered an essential step in understanding and solving the many electrical, geologic and hydrogeological problems of the different aquifers affected by the change in salinity and clay content. Last, it is with an emphasized to show how this variation leads to cover the true values of the hydro-geoelectrical parameters and the accuracy in describing the comparable types of sediments.

Declarations

Conflict of interest The authors declare that they have no conflict of interest.

References

Abd-Elhamid HF, Abdelaty IM, Sherif M (2019) Evaluation of potential impact of Grand Ethiopian Renaissance Dam on Seawater Intrusion in the Nile Delta Aquifer. Int J Environ Sci Technol 16(5):2321–2332. https://doi.org/10.1007/s13762-018-1851-3

Ammar AI (2021) Development of numerical model for simulating resistivity and hydroelectric properties of fractured rock aquifers. J Appl Geophys 189:104319. https://doi.org/10.1016/j.jappgeo.2021.104319

Ammar AI, Gomaa M, Kamal KA (2021) Applying of SP, DC-Resistivity, DC-TDIP and TDEM soundings in high saline coastal aquifer. Heliyon 7(7):e07617. https://doi.org/10.1016/j.heliyon.2021.e07617

Attwa M, Basokur AT, Akca I (2014) Hydraulic conductivity estimation using direct current (DC) sounding data: a case study in East Nile Delta, Egypt. Hydrogeol J 22(5):1163–1178. https://doi.org/10.1007/s10040-014-1107-3

Burger HR, Sheehan AF, Jones CH (2006) Introduction to applied geophysics, exploring the shallow subsurface (**ISBN 0-393-92637**)

Butler SL, Sinha G (2012) Forward modeling of applied geophysics methods using Comsol and comparison with analytical and laboratory analog models. Comput Geosci 42:168–176. https://doi.org/10.1016/j.cageo.2011.08.022

Butler SL, Zhang Z (2016) Forward modeling of geophysical electromagnetic methods using Comsol. Comput Geosci 87:1–10. https://doi.org/10.1016/j.cageo.2015.11.004

CEDARE (2002) Centre for Environment and Development for the Arab Region and Europe (CEDARE) on activities to support African country parties under UNCCD, Cairo. http://water.cedare.int/cedare.int/files15/File2919.pdf

Comsol version 4.4 (2014) Comsol Multiphysics Software (AC/CD module)

Comsol version 5.4 (2018) Comsol Multiphysics Software (AC/CD module)

Dahab KA (1993) Hydrological evaluation of the Nile Delta after the high dam construction. PhD Thesis, Faculty of Science, Monofia University, Egypt, p 30

Ebraheem AM, Senosy MM, Dahab KA (1997) Geoelectrical and hydrogeochemical studies for delineating groundwater contamination due to saltwater intrusion in the northern part of the Nile Delta, Egypt. Ground Water 35(2):216–222. https://doi.org/10.1111/j.1745-6584.1997.tb00077.x

El-Atfy H (2007) Integrated national water resources plan in Egypt. Ministry of Water Resources and Irrigation Alexandria Governorate, Cairo

FAO (2006) World reference base for soil resources. A framework for international classification, correlation and communication. Food and Agriculture Organization, Rome

Farid MS (1980) Nile Delta groundwater study. MSc Thesis, Faculty of Engineering, Cairo University, Giza

Hefny KH (1980) Groundwater in the Nile Valley, Ministry of Irrigation. Report, Water Research Center, Groundwater Research Institute, pp 1–120

Kamal AK (2000) Sea water intrusion the north Nile Delta, Egypt. MSc Thesis, Faculty of Science, Cairo University

Kumar P, Tiwari P, Singh A, Biswas A, Acharya T (2021) Electrical Resistivity and Induced Polarization signatures to delineate the near-surface aquifers contaminated with seawater invasion in Digha, West-Bengal, India. CATENA 207:105596. https://doi.org/10.1016/j.catena.2021.105596

Li Y, Smith RS (2015) Forward modeling of radio imaging (RIM) data with the Comsol RF module. Comput Geosci 85:60–67. https://doi.org/10.1016/j.cageo.2015.08.012

Morsy WS (2009) Environmental, management to groundwater resources for Nile Delta Region. PhD Thesis, Faculty of Engineering, Cairo University, Cairo

MWRI (2013) Adaptation to climate change in the Nile Delta through integrated coastal zone management. Report, Ministry of Water Resources and Irrigation, Giza

Negm AM (ed.) (2019) Groundwater in the Nile Delta, Hdb Env Chem 73:461–486. https://doi.org/10.1007/978-3-319-94283-4. Chapter: Integrated Subsurface Thermal Regime and Hydrogeochemical Data to Delineate the Groundwater Flow System and Seawater Intrusion in the MND, Egypt

RIGW (1980) Safe use studies for groundwater reservoirs in the Nile Delta and Upper Egypt. Research Institute for Groundwater, Cairo

RIGW (1992) Hydrogeologic map of Nile Delta, Scale 1:500,000, 1st edn

RIGW (2002) Nile Delta groundwater modeling. Research Institute for Groundwater, El Qanater El Khayria

Rizzini A, Vezzani F, Coccetta V, Milad G (1978) Stratigraphy and sedimentation of a Neogene: quaternary section in the Nile Delta Area. Mar Geol 27(3–4):327–348. https://doi.org/10.1016/0025-3227(78)90038-5

Rockware (2011) Rockworks software package, Rockworks 15 user manual, Rockware Incorporated

Said R (1981) Geologic evolution of the River Nile. Springer, New York. https://doi.org/10.1007/978-1-4612-5841-4

Said R (1990) The Geology of Egypt. For the Egyptian Gen. Pet. Cor., Conoco Hurghada Inc., And Repsol Exploration, Balkema, Rotterdam Netherlands. https://doi.org/10.1017/s0016756800019828

Sakr SA, Attia FA, Millette JA (2004) Vulnerability of the Nile Delta aquifer of Egypt to seawater intrusion. International conference on water resources of arid and semi-arid regions of Africa. Issues and challenges, Gaborone, Botswana

Sakr SA (2005) Impact of the possible sea level rise on the Nile delta aquifer. A study for Lake Nasser flood and drought control project

(LNFDC/ICC), Planning Sector, Ministry of Water Resources and Irrigation

Saleh MF (1980) Some hydrological and hydro-chemical studies on the Nile delta. MSc Thesis, Faculty of Science, Ain Shams University, Cairo

Salem ZE, Gaame OM, Hassan TM (2008) Using temperature logs and hydrochemistry as indicators for seawater intrusion and flow lines of groundwater in the Quaternary aquifer, Nile Delta, Egypt. In: Proceeding of the 5th international symposium on geophysics, Tanta, Egypt, pp 25–38

Sallouma MK (1983) Hydrogeologic and hydrochemical studies East of Nile Delta, Egypt. Ph.D. Thesis, Faculty of Science, Ain Shams University

Sanuade OA, Amosun JO, Fagbemigun TS, Oyebamiji AR, Oyeyemi KD (2021) Direct current electrical resistivity forward modeling using comsol multiphysics. Model Earth Syst Environ 7:117–123. https://doi.org/10.1007/s40808-020-00898-4

Schlumberger (1984) Geology of Egypt, Paper presented at the Well Evaluation Conference, Schlumberger, Cairo, pp 1–64

Schlumberger, (1995) Well evaluation conference of Egypt. Schlumberger Technical Editing Services, Chester

Serag El Din HM (1989) Geologic, hydrochemical and hydrological studies on the Nile Delta Quaternary aquifer. PhD Thesis, Faculty of Science, Mansoura University, Mansoura

Shata A, El-Fayoumey I (1970) Remarks on the regional geologic structure of the Nile Delta. Bucharest symposium, UNESCO publication chapter, Catalog Number 14859, pp 189–197

Sherif MM (1999) The Nile Delta aquifer in Egypt. In: Bear J, Cheng A, Sorek S, Ouazar D, Herrera A (eds) Seawater intrusion in coastal aquifers, concepts methods and practices. Theory and application of transport in porous media, (14). Kluwer Academic, Dordrecht, pp 559–590. https://doi.org/10.1007/978-94-017-2969-7_17

Sherif MM, Sefelnasr A, Javadi A (2012) Incorporating the concept of equivalent freshwater head in successive horizontal simulations of seawater intrusion in the Nile Delta aquifer, Egypt. J Hydrol 464–465:186–198. https://doi.org/10.1016/j.jhydrol.2012.07.007

Wang X, Yue H, Liu G, Zhao Z (2011) The application of COMSOL multiphysics in direct current method forward modeling. Proc Earth Planet Sci 3:266–272. https://doi.org/10.1016/j.proeps.2011.09.093

Zaghloul Z, Taha A, Hegab O, El Fawal F (1977) The Neogene-Quaternary sedimentary basins of the Nile Delta. Egyptian J Geol 21(1):1–19